Characterisation of tracer distribution in Upper Lake Constance using spatial moments

Markus Wolff

April 24, 2007

Horizontal mixing in Upper Lake Constance was investigated analysing the development of the tracer distribution of conservative tracers simulated using the model ELCOM [3]. In four simulations each including ten different tracer experiments in depths around 3 metres, 30 metres and 60 metres the three-dimensional concentration distributions were calculated for a period of two weeks after release. The method of spatial moments according to *Peeters et al.* [1] was used to analyse the temporal development of the tracer distribution. Therefore mainly the advetive motion of a tracer cloud and the temporal development of the spreading along the principal axes and of the cloud size was considered. In addition, theoretical models for horizontal mixing were tested. It was shown that especially the upper layers - the epilimnion - are important considering horizontal mixing. For tracers injected close to the surface in a distance lager than two kilometres to the shore the method of spatial moments approximated the tracer cloud in a satisfying way during the first week after release. Afterwards and for tracers released close to the shore the approximation was not reliable. After two weeks the cloud sizes ranged in a magnitude between 10 and 32 km^2. Only for tracers released in a central position of Lake Constance a similar behaviour of the growth of the cloud size could be observed during the first week of the experiments. Afterwards and for other release points boundary influences became to strong. Also effects of large scale advective motion showed up after one week. Application of theoretical approaches for horizontal mixing according to *Peeters et al.* [1] showed that a shear diffusion model is able to provide a satisfying description of the behaviour of the cloud for 60% of the tracers injected in central position until day seven after release. This model also accounts for the fact that the tracer clouds were not radially symmetric. The hypothesis that the cloud size grows with elapsed time to the power of 3 according to the inertial subrange model could not be approved. Considering the peak concentration as measure for dilution a concentration of around 0.1% of the initial concentration could be observed for tracers injected into the near-surface layers after two weeks.

Contents

1 Introduction

In lakes the distribution of dissolved and suspended compounds is strongly influenced by the movement of the water [1]. In density-stratified lakes small-scale-turbulence is essential for energy and mass transfer because it brings different water masses in close enough contact to cause mixing by viscosity and diffusivity. The energy however is brought into the system at much larger scales. Relevant mixing processes for any given lake depend on external forcing as well as on lake morphometry. External forces can be river inflow and outflow, turbidity currents, underwater springs, wind, surface heat flux, etc [2]. For Lake Constance especially the wind is important. Mixing has to be differed into horizontal and vertical mixing. Usually, the horizontal mixing is fast compared to the vertical mixing. In large water bodies additionally the effect of large-scale currents occur. Thus the horizontal mixing is a consequence of both the fluctuations of the velocity field and the shear of the mean advective currents ([1],[2]).

Lake Constance is one of the largest alpine lakes in the world and the largest lake in Germany. The basin has a length of 63 kilometres and a maximum width of 14 kilometres and it divides into Upper Lake Constance with a mean water depth of around 100 metres and the much smaller Lower Lake Constance (fig. 1.1). The two parts are hydraulically separated by a channel near the city of Constance. The smaller sub-basin in the north west of Lake Constance is named Lake Überlingen. In this study only Upper Lake Constance is considered, but some attention is also paid to the exchange between the main basin and Lake Überlingen. This is important as one of the big drinking water suppliers in Baden-Württemberg, the "Bodenseewasserversorgung", extracts drinking water for big parts of Baden-Württemberg from Lake Überlingen. To minimise the potential of danger for all kinds of stakeholders by substances that might be released into Lake Constance it is extremely important to know about the behaviour of the transport of such substances.

In this study the horizontal mixing in Upper Lake Constance is investigated. Numerical tracer simulations using the ELCOM model [3] are done and analysed. To simplify and characterise the complex tracer distributions the method of spatial moments is used. Additionally the applicability of theoretical horizontal diffusion models is tested.

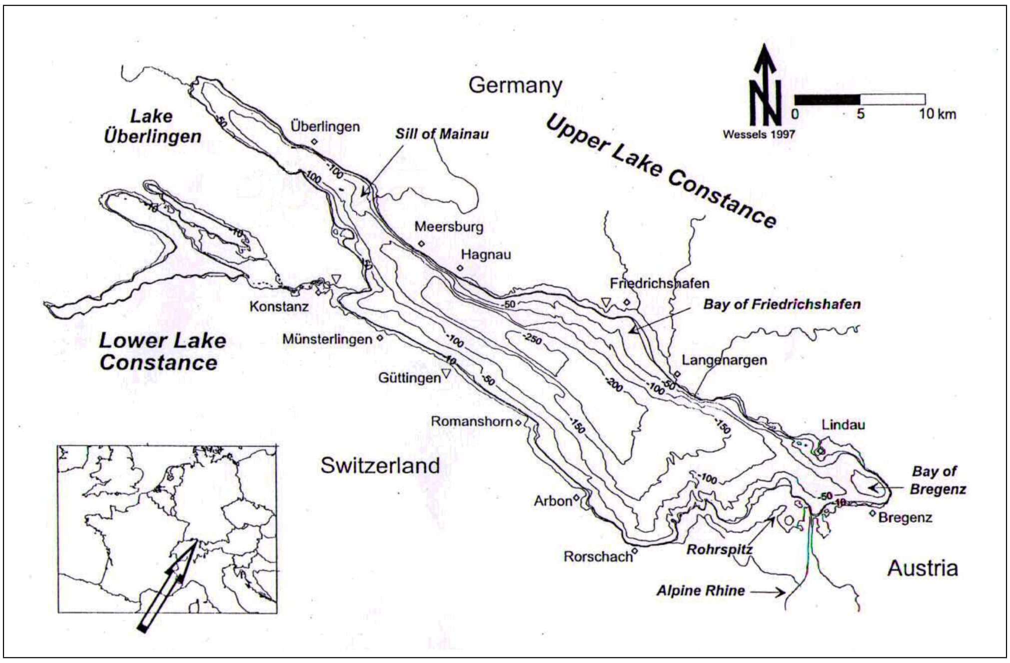

Figure 1.1: Lake constance consisting of Upper Lake Constance, Lower Lake Constance and Lake Überlingen.

2 Used methods and models

2.1 The method of spatial moments

In a lake the movement of a tracer cloud is mainly affected by large scale advection, for example by eddies which are significantly larger than the size of the tracer patch. Eddies that are smaller than the tracer cloud lead to turbulent diffusion and eddies with a size comparable to the tracer cloud cause distortion and stretching of the cloud due to the shear of the velocity field. To describe the behaviour of a tracer cloud its transport can be separated into advective and diffusive transport, where the movement of its centre of mass (x_s, y_s, z_s) is the advective part and the change of the cloud shape relative to the centre of mass the diffusive part. The distribution can then be characterised by quantities such as the total Mass M_0, the coordinates of the centre of mass x_i, and variance and covariance $\sigma_{x_i x_j}$:

$$M_0(t) = m(t) = \iiint c(x, y, z, t)\,\mathrm{d}x\,\mathrm{d}y\,\mathrm{d}z, \tag{2.1}$$

$$M_{1_i}(t) = x_{i_s}(t) = \frac{1}{M_0} \iiint x_i c(x, y, z, t)\,\mathrm{d}x\,\mathrm{d}y\,\mathrm{d}z, \tag{2.2}$$

$$M_{2_{ij}}(t) = \sigma_{x_i x_j}(t) = \frac{1}{M_0} \iiint (x_i - x_{i_s})(x_j - x_{j_s}) c(x, y, z, t)\,\mathrm{d}x\,\mathrm{d}y\,\mathrm{d}z. \tag{2.3}$$

Herein $i, j = 1, 2, 3$, x_i are the Cartesian coordinates ($x_1 = x$, $x_2 = y$, $x_3 = z$) and $c(x, y, z, t)$ is the spatial time dependent concentration field. Moments of higher order are not considered here, which means that the information of the concentration distribution is reduced to that of a three-dimensional normal distribution. As neither the total mass - for conservative tracers - nor the movement of the centre of mass is influenced by mixing processes the only variables that are left describing the mixing are the variances and covariances. In consequence the mixing process is then solely described by the temporal change of $\sigma_{x_i x_j}$. If a lake is stratified, the vertical mixing can be assumed to be small compared to the horizontal mixing. Thus, the vertical mixing can be neglected. The validity of this assumption will be looked at later in chapter 4. To analyse horizontal mixing the concentration distribution is integrated vertically. This leads to a two-dimensional distribution for which the following 2^{nd} order moments are relevant:

$$M_2(t) = \begin{pmatrix} \sigma_{xx}(t) & \sigma_{xy}(t) \\ \sigma_{yx}(t) & \sigma_{yy}(t) \end{pmatrix}. \tag{2.4}$$

The spreading of a tracer cloud is often highly anisotropic. After rotating the coordinate system in a way that the x and y axes coincide with the major and minor principal axes of the distribution, the corresponding variances are σ^2_{ma} and σ^2_{mi}, whereas the covariances become zero. In practice this means that the variances along the principal axes σ^2_{ma} and σ^2_{mi} are the eigenvalues of the matrix $M_2(t)$ (eq. 2.4) and the directions of the principal axes are the directions of the eigenvectors of $M_2(t)$. Thus, the horizontal extent of the vertically integrated concentration distribution (in other words the size of a tracer cloud) can be defined as

$$\sigma^2 = 2\sigma_{ma}\sigma_{mi}. \tag{2.5}$$

Eq. 2.5 can then be used for example to estimate the horizontal diffusivity like

$$\frac{d\sigma^2}{dt} = 4K_{app}, \tag{2.6}$$

as the instantaneous rate of mixing can be characterised by an apparent horizontal diffusion coefficient K_{app} that is related to the temporal evolution of σ^2([1],[2]).

2.1.1 Application to discrete data

The numerical experiments which will be described later (chapter 3.2) yield to three-dimensional concentration distributions for the single tracers for a large domain and for many time steps. This represents a huge amount of discrete data from which it is not so easy to appraise the movement and spreading of the tracer distributions. One possibility of a simplification of these data for analysis is the use of spatial moments. Therefore, the method of spatial moments described above (section 2.1) is adapted for discrete distributions as follows:

$$M_0(t) = m(t) = \sum_{k=1}^{n_{cells_k}} \sum_{j=1}^{n_{cells_j}} \sum_{i=1}^{n_{cells_i}} [c_{ijk}(t)\,\Delta x_i\,\Delta y_j\,\Delta z_k], \tag{2.7}$$

$$M_{1_m}(t) = x_{m_s}(t) = \frac{1}{M_0} \sum_{k=1}^{n_{cells_k}} \sum_{j=1}^{n_{cells_j}} \sum_{i=1}^{n_{cells_i}} [x_{m_{ijk}} c_{ijk}(t)\,\Delta x_i\,\Delta y_j\,\Delta z_k], \tag{2.8}$$

$$M_{2_{ml}}(t) = \sigma_{x_m x_l}(t) = \frac{1}{M_0} \sum_{k=1}^{n_{cells_k}} \sum_{j=1}^{n_{cells_j}} \sum_{i=1}^{n_{cells_i}} [(x_{m_{ijk}} - x_{m_s}(t)) (x_{l_{ijk}} - x_{l_s}(t)) c_{ijk}(t)\,\Delta x_i\,\Delta y_j\,\Delta z_k], \tag{2.9}$$

where i, j, k are the indices of the cells in x-, y-, and z-direction, n_{cells} is the number of cells in each direction and x_m and x_l are the cartesian coordinates for x (l, $m = 1$), y (l, $m = 2$) and z (l, $m = 3$). If horizontal mixing is assumed to be the main mixing process and vertical mixing can be neglected, then l, $m = 1$, 2 in equation (2.9).

2.2 Models for horizontal diffusion

Theoretical models which describe horizontal diffusion in lakes are almost all of empirical origin. They model the temporal change of statistical properties (e. g. the variance) of a concentration distribution as a descriptive value for the cloud size. The basis of the different approaches are the properties of the velocity field that are assumed to be important for the horizontal mixing process. In the following, a brief review based on [1] and [2] will be given.

One possible approach for turbulence in an ocean or lake is the inertial subrange model. If the assumption is made that the cloud size ranges within the scales of the inertial subrange of the turbulence spectrum, similarity theory predicts that the cloud size will grow proportional to t^3. The spreading of the cloud size should also depend on the intensity of the turbulence, which can be measured by the rate of dissipation ε. Together that leads to the equation

$$\sigma^2 = \text{const}\, \varepsilon t^3. \tag{2.10}$$

In this model the velocity field is assumed to be three dimensional and therefore the statistical properties to be spherical symmetrical. It is clear that turbulence as the most important process for mixing is always three-dimensional. However, vertical turbulence is often limited by vertical density stratification or limited vertical size of a water body. Therefore, it is important that equation (2.10) also remains valid for two-dimensional isotropic turbulence if the cloud size is within the inertial subrange. Using the inertial subrange approach (eq. 2.10) together with equation (2.6), a horizontal diffusivity can be calculated as

$$K_{app} = \text{const}\, \varepsilon^{1/3} \sigma^{4/3}. \tag{2.11}$$

The mathematical form of equation (2.10) suggests using the power law

$$\sigma^2 = \text{const}\, t^m, \tag{2.12}$$

as a more general approach, leading, together with equations (2.6) and (2.12), to the corresponding horizontal diffusion coefficient

$$K_{app}(\sigma) = \text{const}\, \sigma^{2(1-1/m)}. \tag{2.13}$$

It has to be mentioned that in these models the size of the tracer cloud is equal to zero ($\sigma^2 = 0$) for $t = 0$. This means that if the initial tracer cloud has a finite size, $t = 0$ is the hypothetical time when the cloud size could have been zero. Therefore, a more general form would be expressed by

$$\sigma^2 = \text{const}\, (t + t_0)^m \tag{2.14}$$

where t_0 is a function of the initial cloud size at $t = 0$ and $\sigma_0^2 = \text{const}\, t_0^m$.
The empirical approach of the inertial subrange model (eq. 2.10) has also been investigated in several series of experiments, *Peeters et al.* [1] refer to *Okubo* [1971] for instance.

As further development *Peeters et al.* [1] mention the modification by *Joseph and Sendner*. Their assumption was that the distance between an individual water parcel and the centre of mass of a tracer distribution increases on average with a constant velocity which leads to an exponent in equation (2.12) of $m = 2$. The effective diffusivity then increases linearly in time.

Finally, for exponent $m = 1$ in equation (2.12) the diffusivity would become constant according to the Fickian law. Thus all together the mentioned models cover a general power law (eq. 2.12) with a range for m lying between 1 and 3.

One restriction of all these models is the radial symmetric behaviour. To describe non-radial distributions as they appear in most experimental results, shear diffusion models were developed. Especially *Carter and Okubo* is referred to for this situation by *Peeters et al.* [1]. The underlying assumption of shear diffusion models is that the velocity field can be separated into two parts. One part contains the turbulent fluctuations and the other the large-scale advective flow. The small-scale turbulence is assumed to follow the Fickian law. It is expressed by the small-scale horizontal diffusivity K_h that is further assumed to be homogeneous ($K_x = K_y = K_h$) and by the diapycnal diffusivity K_d. With the further assumption that the non-turbulent velocity field is along the x axis with the simple form $u = ay + bz$, the variances in major and minor directions of a tracer cloud can be expressed as

$$\begin{aligned}\sigma_{ma}^2 =& 2K_h t + \frac{1}{3}(a^2 K_h + b^2 K_d)t^3 + \\ & \sqrt{K_h^2 a^2 t^4 + [\frac{1}{3}(a^2 K_h + b^2 K_d)t^3]^2}, \\ \sigma_{mi}^2 =& 2K_h t + \frac{1}{3}(a^2 K_h + b^2 K_d)t^3 - \\ & \sqrt{K_h^2 a^2 t^4 + [\frac{1}{3}(a^2 K_h + b^2 K_d)t^3]^2},\end{aligned} \tag{2.15}$$

and the tracer cloud size σ^2 according to equation (2.5) as

$$\sigma^2 = 2\sqrt{4K_h^2 t^2 + \frac{1}{3}K_h(a^2 K_h + 4b^2 K_d)t^4}. \tag{2.16}$$

For the case of zero velocity shear (a = 0, b = 0) the development of the cloud size behaves like $\sigma^2 = 4K_h t$ which is the solution of equation (2.6) for constant diffusivity (Fickian diffusion). For larger time scales the increase of σ^2 is proportional to t^2 comparable to the *Joseph and Sendner* model whereas the model of *Carter and Okubo* is able to describe non-radially symmetric distributions by σ_{ma}^2 and σ_{mi}^2 which are usually different. Actually, this model predicts that $\sigma_{ma} \sim t^3$ and $\sigma_{mi} \sim t$ for long diffusion times. The major principal axis of the tracer cloud then turns into the direction of the current ([1],[2]). There are also other shear-diffusion models, but they will not be further considered in this study.

3 Simulation

3.1 The computational model - ELCOM

The Estuary, Lake and Coastal Ocean Model – ELCOM – that is used for this study is a three-dimensional hydrodynamics model for lakes and reservoirs. It can be used to predict the variation of water temperature, salinity or transport of tracer or drifters in space and time [3].
It computes a model time step in a staged approach consisting of

1. Introduction of surface heating/cooling in the surface layer,
2. Mixing of scalar concentration and momentum using a mixed-layer model,
3. Introduction of wind energy as a momentum source in the wind-mixed layer,
4. Solution of the free-surface evolution and velocity field,
5. Horizontal diffusion of momentum,
6. Advection of scalars, and
7. Horizontal diffusion of scalars.

As fundamental numerical scheme the ELCOM-Manual [3] names the TRIM approach of *Casulli and Cheng* [1992], which was adapted with some modifications.
For transport of momentum an unsteady Raynolds-averaged Navier-Stokes (RANS) equation is used. The transport equations for both scalars and momentum use the Boussinesq approximation and neglect the non-hydrostatic pressure terms. The free surface evolution is governed by a vertical integration of the continuity equation applied to the Reynolds-averaged kinematic boundary condition [3].

3.2 Setting and conditions

In this study ELCOM is applied to Lake Constance. As Lake Constance is large, the effects of the Coriolis force have to be considered for the modelling as well as density effects due to temperature differences. As closure scheme for the turbulence modelling the wind-mixed layer model is used [3]. Influences of surface thermodynamics and inflow or outflow – here especially the river Rhine – are neglected to save computational time. As main driving force a uniform wind-field with the wind coming from a north east direction with a speed of 3 metres per second is used. The lake is assumed to be stratified like in late summer and an according initial vertical temperature profile is set (fig. 3.2). As can be seen for example in figure 3.1 Lower Lake Constance (the south west part) is not considered. That is because Lower Lake Constance is not hydrodynamically coupled to Upper Lake Constance and can therefore be ignored for the simulation of Upper Lake Constance to save computational time. In each run ten

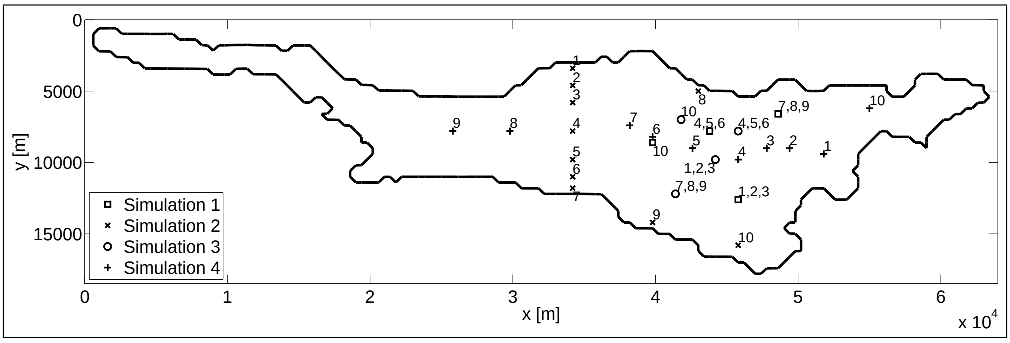

Figure 3.1: Locations of tracer releases into Lake Constance in the different numerical experiments with the numbers of tracers from 1 to 10.

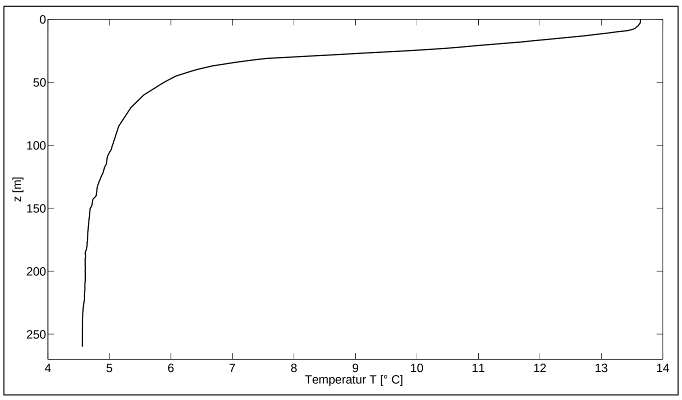

Figure 3.2: Vertical initial temperature profile for the simulations

Depth [m]	Simulation	Tracer
2.5 - 5	1	1-10
	2	1, 4, 7, 10
	3	1, 4, 7, 10
	4	1-10
30-35	1	-
	2	2, 5, 8
	3	2, 5, 8
	4	-
60	1	-
	2	3, 6, 9
	3	3, 6, 9
	4	-

Table 3.1: Depth of the tracer release points.

conservative tracers are released simultaneously at different positions (fig. 3.1). The release positions differ not only in x- and y- direction, but for some points also in the z-direction. For most of the tracers the release depth lies close to the surface between 2.5 and 5 meters, for some at around 30 meters which is approximately at the deeper end of the metalimnion and for some at around 60 meters, within the hypolimnion (table 3.1). Although a point-like instantaneous injection is aimed for, it has to be kept in mind that for reasons of discretisation the tracer is always released in a whole cell, which means in a volume of 400 m x 400 m x 2.5 m and over 1.92 hours which are 36 time steps. Ideally the tracer would be released in one time step which means for 240 seconds but for numerical reasons no shorter time interval could be chosen. The simulated time is 28 days. Because the simulations start form rest ($\mathbf{u} = 0$) the velocity field takes some time to develop. After two weeks of simulated time it is assumed to be well developed and so the tracer is released at day 15 of the simulation. However, comparing the velocity fields shown in figures 3.3 and 3.4 it can be realized that there is still a lot of development between day 15 and day 28 both in direction and magnitude of the single velocity vectors. This has to be considered for the interpretation of the results (chapter 4).

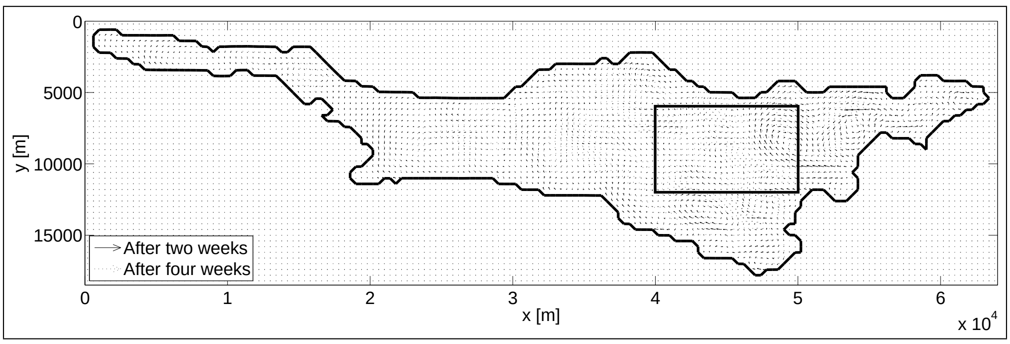

Figure 3.3: The velocity field after two weeks and after four weeks of simulated time where the Box shows the area of detail in figure 3.4

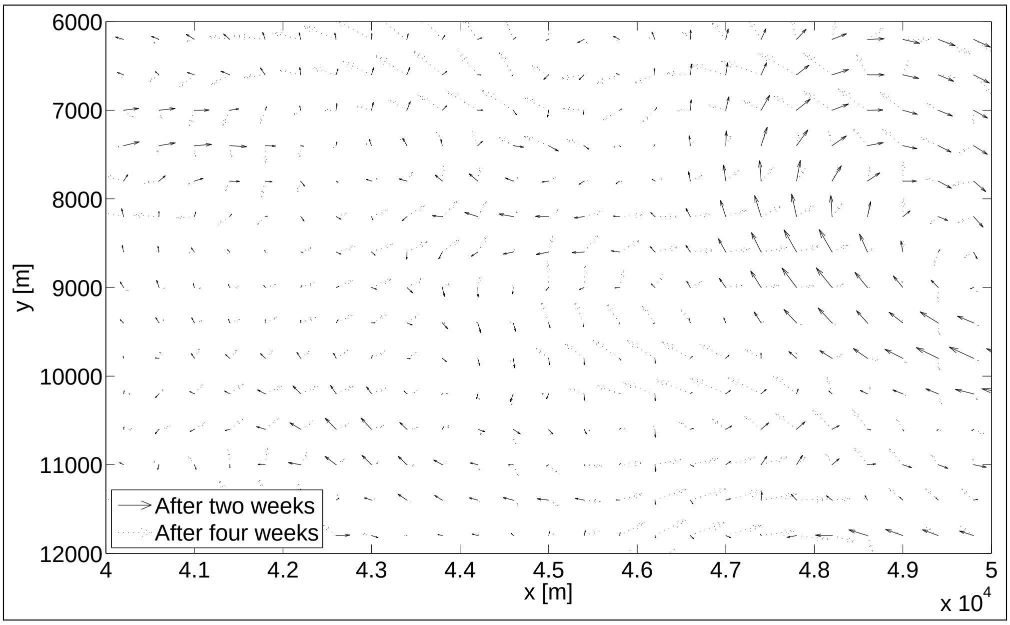

Figure 3.4: The velocity fields after zooming into the marked area of fig. 3.3.

4 Results and discussion

Several simulations for Lake Constance as described in the previous chapter yielded to three-dimensional concentration distributions for the single tracers for the whole lake and for every time step. To analyse this huge amount of data the method of spatial moments as described in chapter 2.1 is used. For the application of the moment analysis a matlab program was written using equations 2.7, 2.8, 2.9, 2.4 and 2.5. In this chapter the results of the different simulations are at first analysed concerning the movement of the centre of mass and the spreading of the tracer clouds aiming at finding a characteristic behaviour. Afterwards, the behaviour of the cloud size over time is analysed especially concerning boundary influences. Furthermore, the validity of horizontal diffusion models as described in chapter 2.2 is investigated and finally the relevance of dilution is considered.

4.1 Movement of the centre of mass

In chapter 2.1 it was explained that the movement of the centre of mass can be interpreted as the advective part of the tracer transport. Therefore, it seems reasonable to have a closer look at the velocity field before analysing the first moment. As already mentioned in chapter 3.2, the velocity field is assumed to be fully developed after day 15 when the tracer is injected. Furthermore, it was seen that there is a considerable change in the horizontal velocity field between day 15 and day 28. No attention is paid to the vertical velocity component as it is assumed to be small compared to the horizontal component in a well stratified lake and does not influence the mixing process. Figure 4.1 shows the horizontal velocity field of layer 43 of the computational mesh, which lies in a depth of approximately 2.5 to 5 metres, after 15 days. As can be seen up to that point larger scale motions – scale of the lake – just begin to develop. Smaller scale eddies up to a size of 1 to 5 kilometres are already generated. After 19 days (fig. 4.2) larger scale flow becomes more noticeable and the magnitude of the velocities gets higher. On day 28, motions of the scale of half the lake can be seen (fig. 4.3) composed by smaller eddies building some kind of circulation. There are two possible explanations for the described changes in the velocity field. One is that the flow field is not fully developed after two weeks of simulated time. The second possibility is a change due to internal waves as investigated for Lake Constance by *Appt* [4]. In this work it is also reported that after 8 days of simulated time the initial conditions are not relevant any longer.
Another difference can be seen by comparing figure 4.3 to figure 4.4. At some locations the main flow direction from a depth of around five metres and downwards seems to be reverse to the flow direction in a depth smaller than five metres. This effect becomes even stronger comparing the flow in a depth of between 7.5 and 10 metres to the flow at the surface. Altogether it can be noticed that the flow situation in Lake Constance is very complex.

Figure 4.5 shows the vertical movement of the centres of mass of simulation 1. The

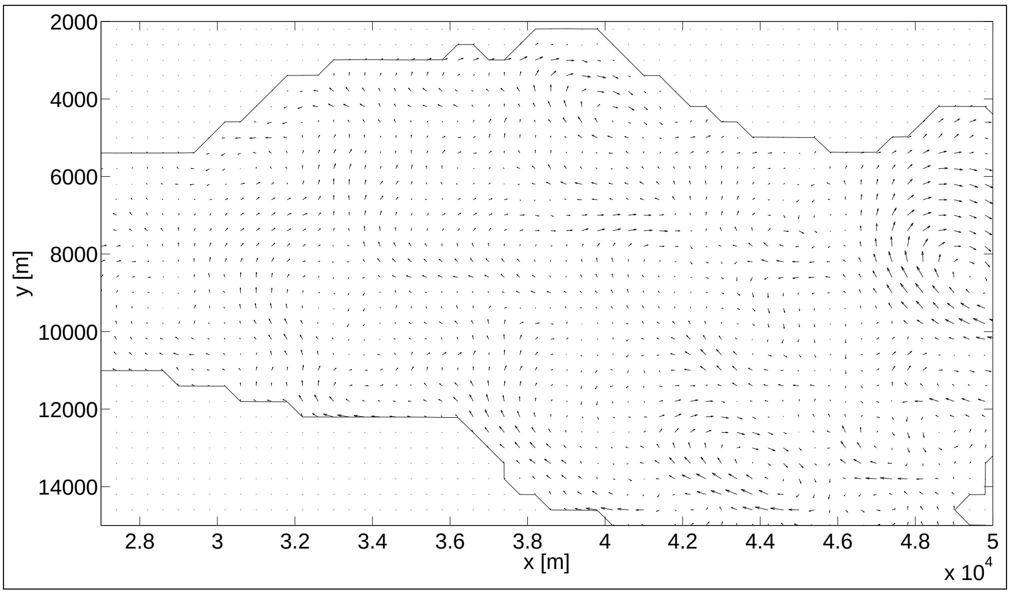

Figure 4.1: The horizontal velocity field after 15 days in between 2.5 and 5 metres depth.

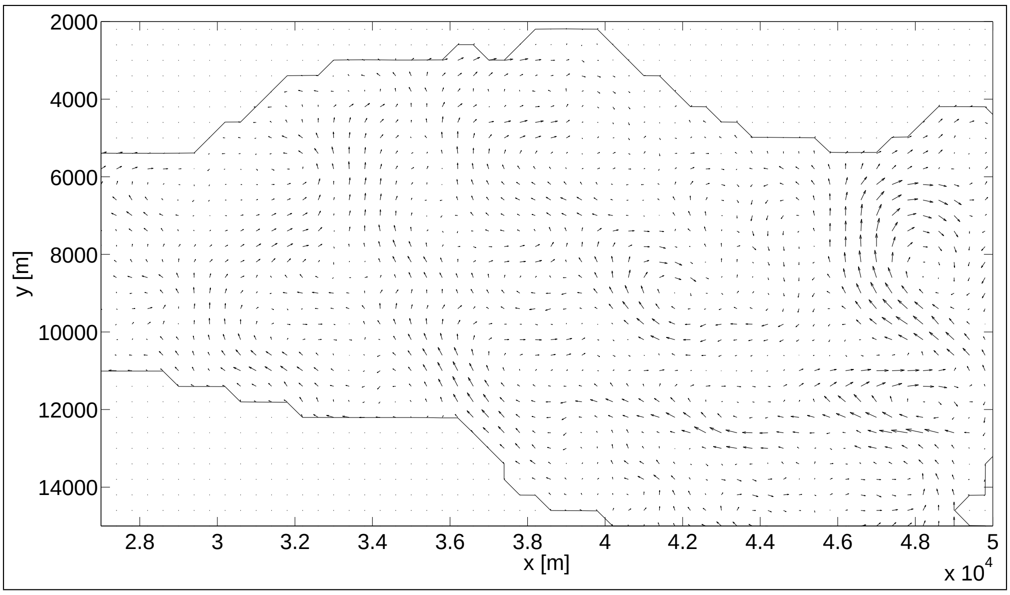

Figure 4.2: The horizontal velocity field after 19 days in between 2.5 and 5 metres depth.

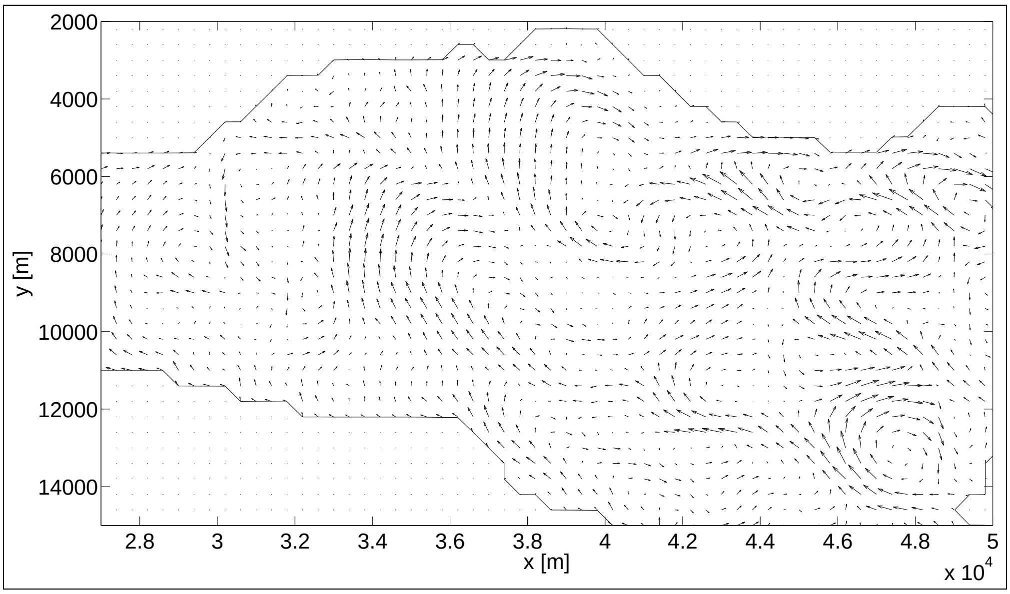

Figure 4.3: The horizontal velocity field after 27 days in between 2.5 and 5 metres depth.

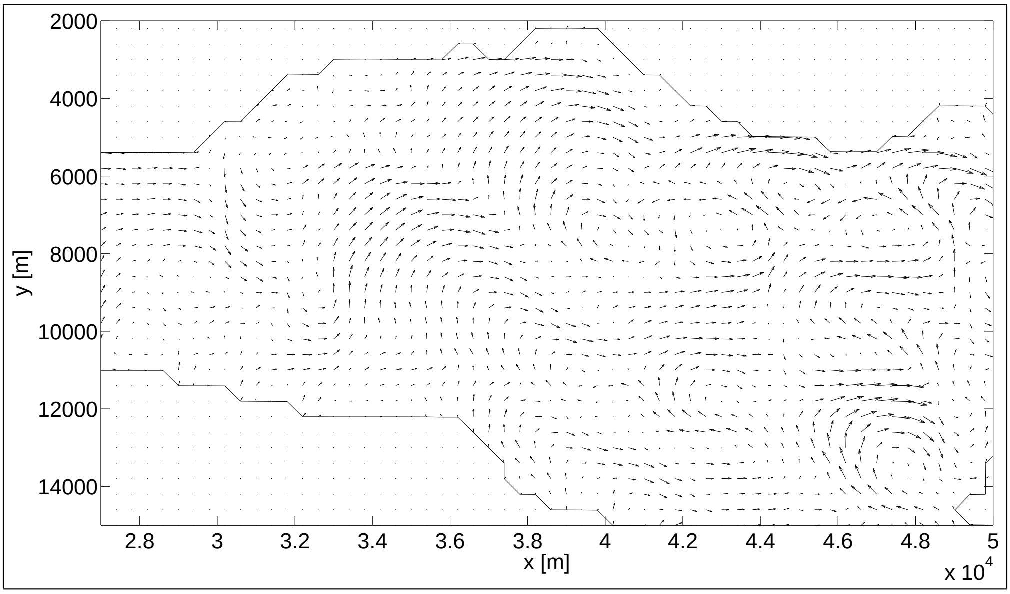

Figure 4.4: The horizontal velocity field after 27 days in between 5 and 7.5 metres depth.

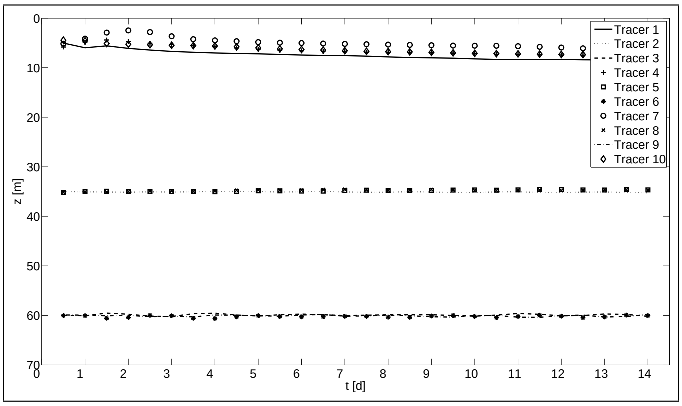

Figure 4.5: The vertical movement of the centre of mass of the tracers distribution of simulation 1.

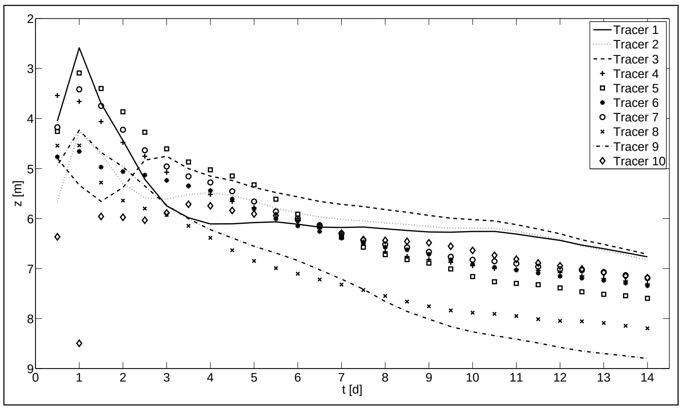

Figure 4.6: The vertical movement of the centre of mass of the tracers distribution of simulation 4.

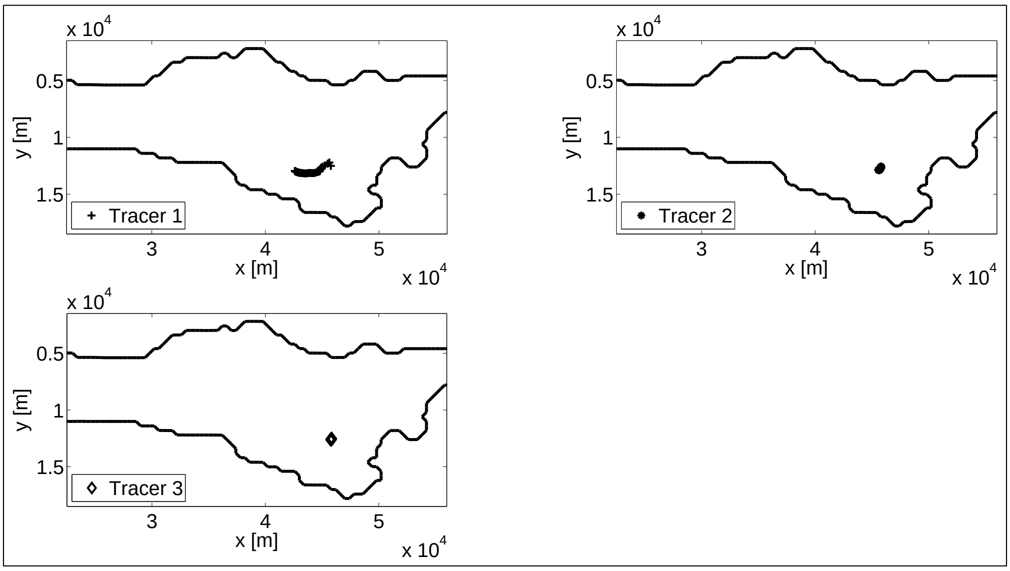

Figure 4.7: The horizontal movement of the centre of mass of a tracer released in three different depths (simulation 1).

tracer is injected into the lake at three different depths here (table 3.1). As can be seen there is almost no vertical movement in the two deeper areas, where no vertical exchange should take place. Close to the lake surface only little vertical movement is visible. The behaviour at the surface can be demonstrated better in figure 4.6 where all the tracers are released into an upper layer. The centre of mass ranges from a depth of 3 metres to a depth of 8 metres, which is approximately the same as in the other simulations. These results show that the vertical exchange in a well-stratified lake is small compared to horizontal movement which can be on the order of several kilometres (fig. 4.9). Thus the assumption of horizontal advection is justified and from now on only the horizontal change of the centre of mass will be analysed considering the mixing process.

As mentioned above, n deeper areas the centre of mass undergoes little to no vertical motion. But usually there should be almost no flow and only little transport in the deeper layers at all. Figures 4.7 and 4.8 show that in a depth of around 60 metres there is no recognisable change in the horizontal position of the centre of mass, whereas close to the surface, movement on the order of kilometres occurs. At a depth of around 30 metres a change of the position of the centre of mass is visible depending on the location in the lake but it is still small compared to the movement in the upper layers. So for an investigation of the horizontal mixing processes in Lake Constance especially the near surface layers of the epilimnion are important. The movement of the centres of mass of a series of tracers released in the near surface layers are shown in figures 4.9 and 4.10. As can be seen the main direction of the movement appears to be from the south east to the north west which is reasonable as it is the direction of the main driving force, namely the wind.

After having taken a look at the flow field at the beginning of this chapter, the question comes up now if the movement of the centre of mass can be directly linked to the flow around it. To answer this, one of the transported tracers will be described in more detail as an example. Figure 4.11 shows an enlarged section of fig. 4.10, figures

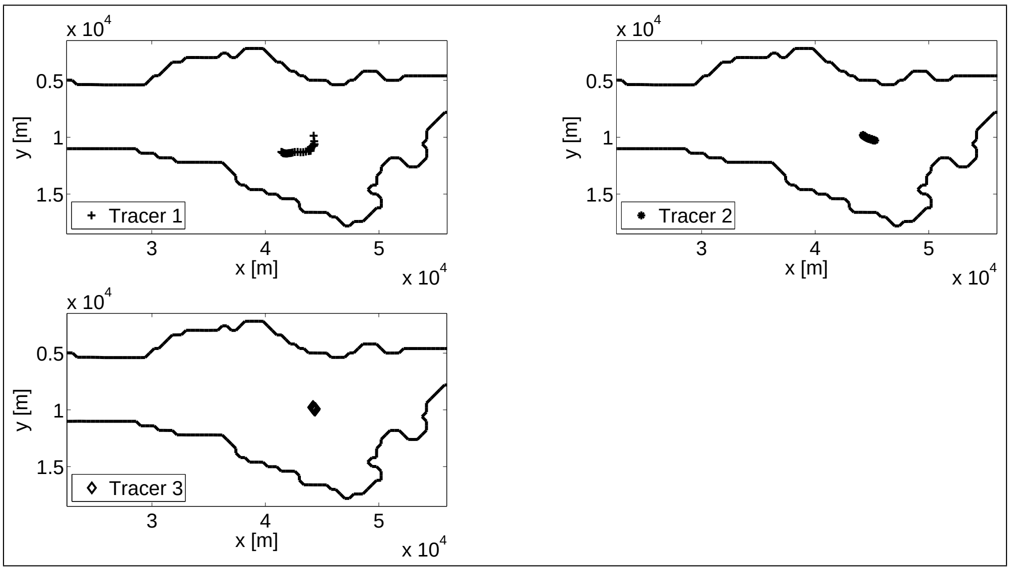

Figure 4.8: The horizontal movement of the centre of mass of a tracer released in three different depths (simulation 3).

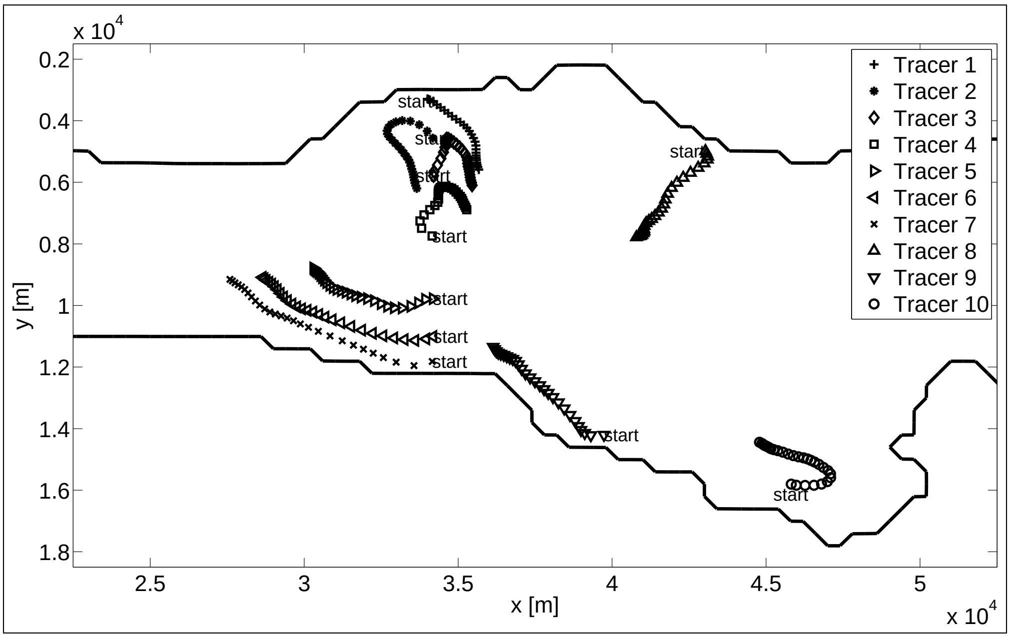

Figure 4.9: The horizontal movement of the centres of mass of the tracers released in simulation 2.

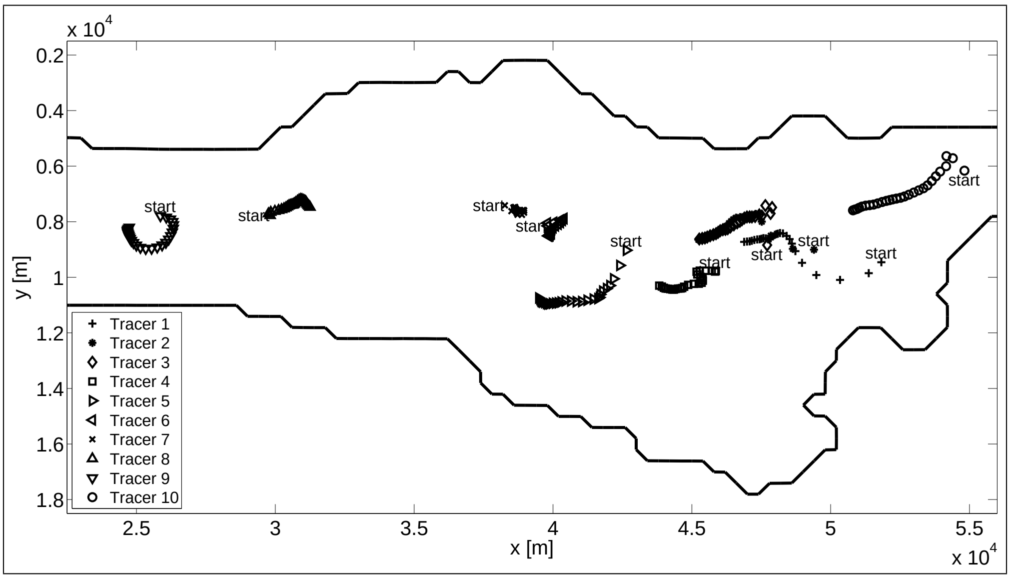

Figure 4.10: The horizontal movement of the centres of mass of the tracers released in simulation 4.

4.12, 4.13 and 4.14 show the corresponding section of the horizontal velocity fields. From figure 4.6 it arises that after approximately 5 days all the centres of mass are below a depth of 5 metres. For most of the tracers the centres of mass stay in a depth between 5 and 7.5 metres till the end of the simulation, a few even go deeper than 7.5 metres. So for the first days the centre of mass shown in figure 4.11 has to be related to the velocity field of figure 4.12, afterwards to the velocity fields of figure 4.13 and figure 4.14, respectively. As can be seen easily there is no obvious relationship between the movement of the centre of mass and its directly surrounding flow if the situation is as complex as in Lake Constance. It always has to be kept in mind that the centre of mass is a quantity resulting from a spatial averaging process. Thus, an evaluation of the change of the centre of mass in connection with the flow situation of Lake Constance can only be done considering the whole area of a tracer cloud. The movement of the centre of mass can then be interpreted as the average advective motion of the whole tracer cloud according to the theory of spatial moments (ch. 2.1) but it is not the path along which a tracer particle would be transported advectively directly due to the local flow. For Lake Constance this implies also that one can not just look at the local velocity field to estimate the movement of a tracer cloud.

4.2 Spreading

The diffusive-dispersive part of the tracer transport can be represented by the second moment (eq. 2.9, 2.3) as described in chapter 2.1. The complex flow situation of Lake Constance as discussed in section 4.1 is expressed more clearly by the process of spreading (ch. 4.2) than by the movement of the centre of mass, although changes in the position of the centre of mass are certainly always influenced by the spreading of a tracer cloud (ch. 2.1).

Figure 4.15 shows the results of the calculation of the second moment for a chosen tracer. Using the method of spatial moments a Gaussian shape of the tracer cloud is

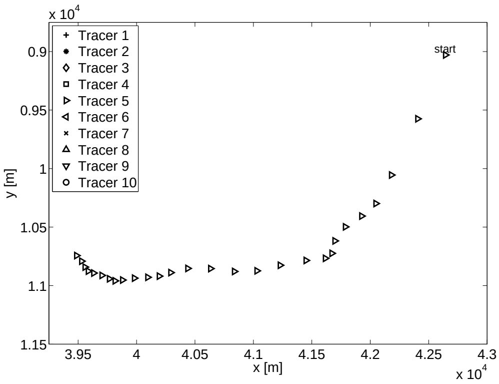

Figure 4.11: The horizontal movement of the centres of mass of tracer 5 of simulation 4.

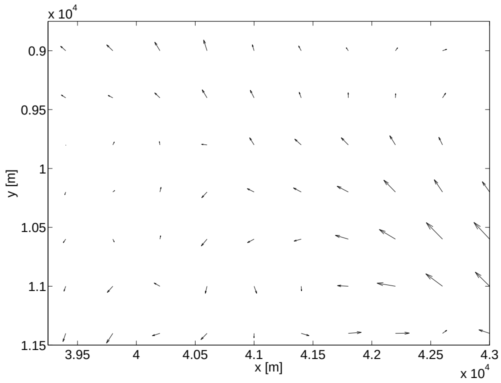

Figure 4.12: Enlarged section of the velocity field at day 15 in a depth between 2.5 and 5 metres.

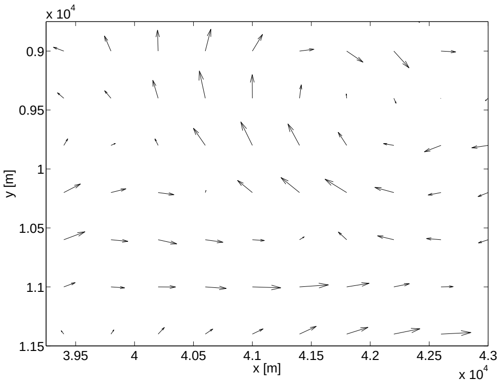

Figure 4.13: Enlarged section of the velocity field at day 19 in a depth between 5 and 7.5 metres.

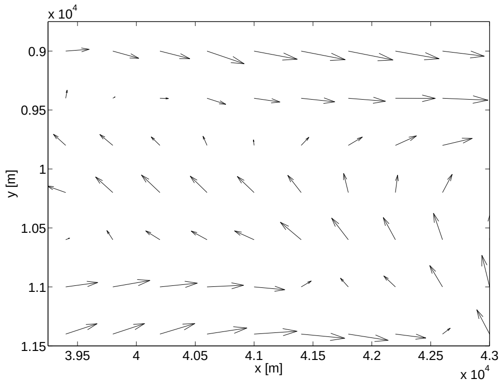

Figure 4.14: Enlarged section of the velocity field at day 23 in a depth between 5 and 7.5 metres.

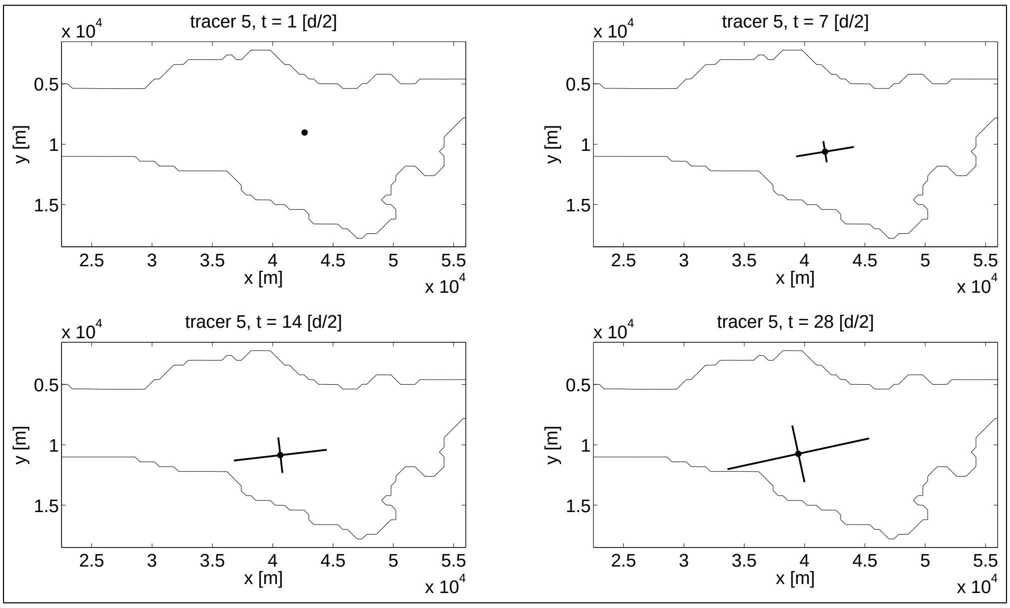

Figure 4.15: Horizontal spreading of tracer 5 of simulation 4 in major and minor direction around the centre of mass.

assumed. The horizontal spreading in the major and minor axis around the centre of mass is symbolised by a cross. As can be seen, after 14 days of simulated time the horizontal spreading ranges between 10 and 15 kilometres in the major direction and around five kilometres in the minor direction. In contrast, the vertical spreading that can be seen in figure 4.16 is on the order of few metres (here around ten metres). Thus the vertical spreading can be neglected considering the mixing process as it is very small compared to the horizontal mixing. A different case can be seen in figure 4.17. Tracer 4 is released close to the surface, tracer 5 in a depth of around 30 metres and tracer 6 at around 60 metres. The figure shows that not only the movement of the centre of mass of tracers released in deeper layers is very small compared to tracers released next to the surface but also the spreading. So again it can be pointed out that for an investigation of the horizontal mixing processes in Lake Constance especially the near surface layers of the epilimnion are important. Usually the method of spatial moments shows the best results if there are no or minimal influences of boundaries which are represented by the lake shore here. Therefore, the next section (4.3) will deal with the applicability of the method of spatial moments for Lake Constance.

4.3 Applicability of the moment analysis

For the application of the method of spatial moments some assumptions have to be looked at again at first. It is assumed that in a well stratified lake the vertical mixing is negligible small compared to the horizontal mixing. This was shown to apply for the results of the computational experiments for Lake Constance in the previous sections (chs. 4.1 and 4.2). Another assumption concerning especially the results of the computation using ELCOM is that the velocity field starting from $\mathbf{u} = 0$ is sufficiently developed when the tracer is injected. Here two weeks of simulated time are used for start-up. But as already described in section 4.1 there is still a lot of change

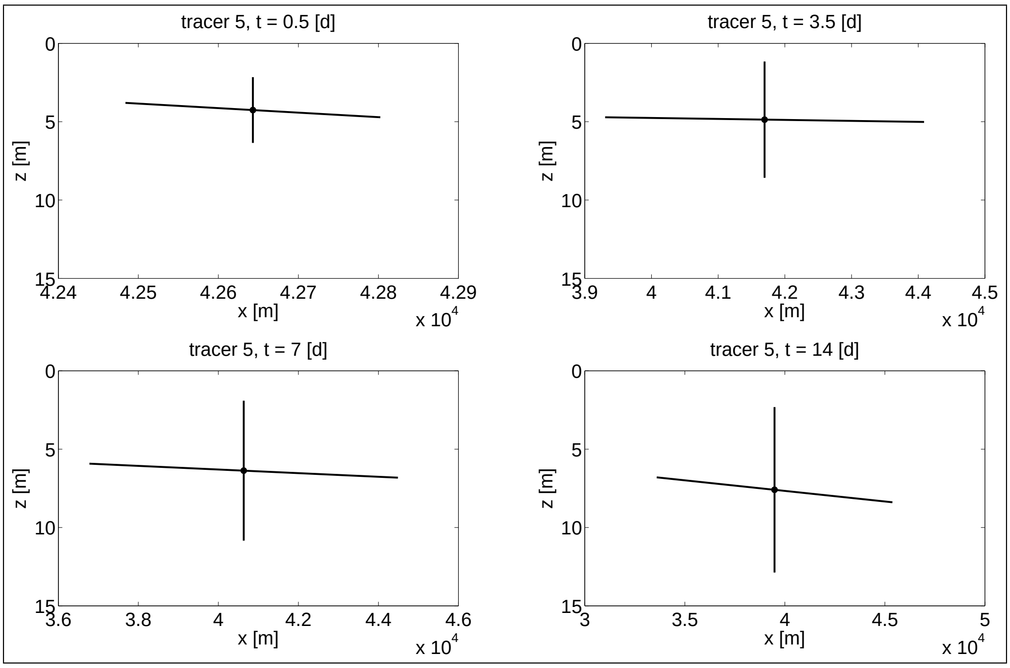

Figure 4.16: Spreading of tracer 5 of simulation 4 in major and minor direction around the centre of mass in the x-z-plane.

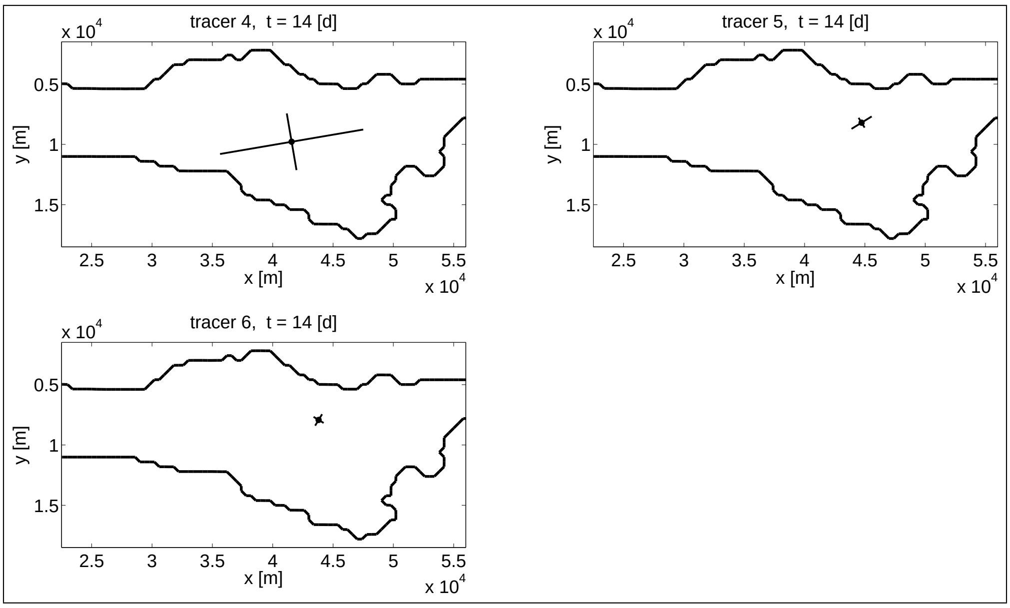

Figure 4.17: Spreading of tracer 4,5 and 6 of simulation 1 in major and minor direction around the centre of mass after 14 days.

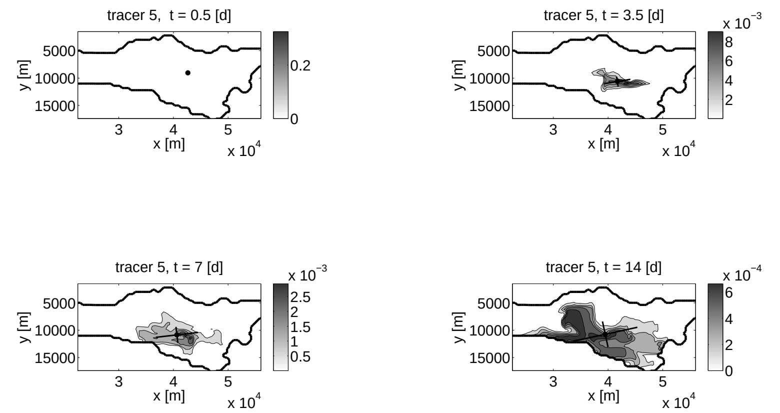

Figure 4.18: Spreading of tracer 5 of simulation 4 in major and minor direction around the centre of mass and concentration field for different time steps.

in the velocity field from the time the tracer is released until the end of the simulation. This could be due to a too short start-up time or due to internal waves (ch. 4.1). But referring to *Appt* [4] the flow field including the internal wave motion should be sufficiently well developed after 8 days. The internal waves are then the main reason for the fluctuations of the velocity field. Therefore, the results can be used for further analysis of the situation of Lake Constance.

Concerning the movement of the centre of mass it has been shown above that it cannot be directly linked to the flow field in Lake Constance as this is much too complex. It now has to be determined whether the moment analysis represents a sufficiently good approximation of a tracer distribution in Lake Constance including the movement of the centre of mass as an averaged advective motion and the stretching and spreading of the cloud expressed by the second moment. Therefore, the spreading around the centre of mass as calculated from the spatial moments is plotted together with the concentration distribution resulting from the simulation. Several tracers resulting from different simulations each representing a characteristic situation in the lake are chosen for the comparison.

Figures 4.18 to 4.20 show tracer experiments with the release points located in a central position to obtain a maximum distance to the shore. At first it has to be mentioned that all three tracer clouds reach the shore within the simulated time. Especially in figure 4.18 the development of the cloud seems to be noticeably influenced by the shore. From the shape of the concentration distribution also the complex flow situation can be derived. In figure 4.19 the cloud after 14 days is stretched forming some kind of circle. This might be due to a large scale eddy. In figure 4.20 the tracer distribution even becomes separated into two parts. This seems to be due to large scale currents flowing in opposite directions. All the effects mentioned before produce problems for the use of spatial moments. The elliptic shape of the cloud around the centre of mass that is assumed here is not able to reproduce the complicated patterns of the concentration distributions and partly not even able to catch the area of the highest concentrations (figs. 4.19 and 4.20, day 14). One week after the tracer release the described effects

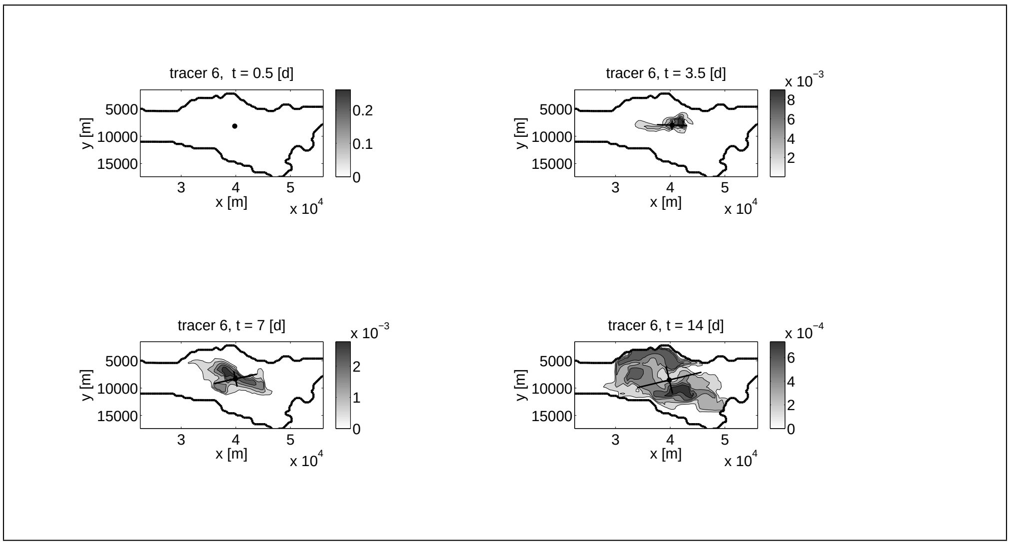

Figure 4.19: Spreading of tracer 6 of simulation 4 in major and minor direction around the centre of mass and concentration field for different time steps.

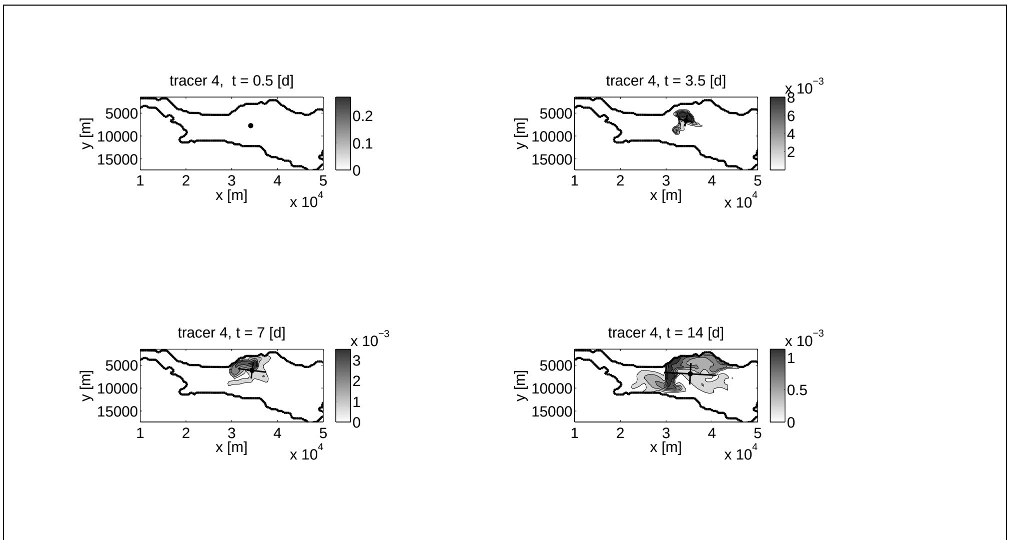

Figure 4.20: Spreading of tracer 4 of simulation 2 in major and minor direction around the centre of mass and concentration field for different time steps.

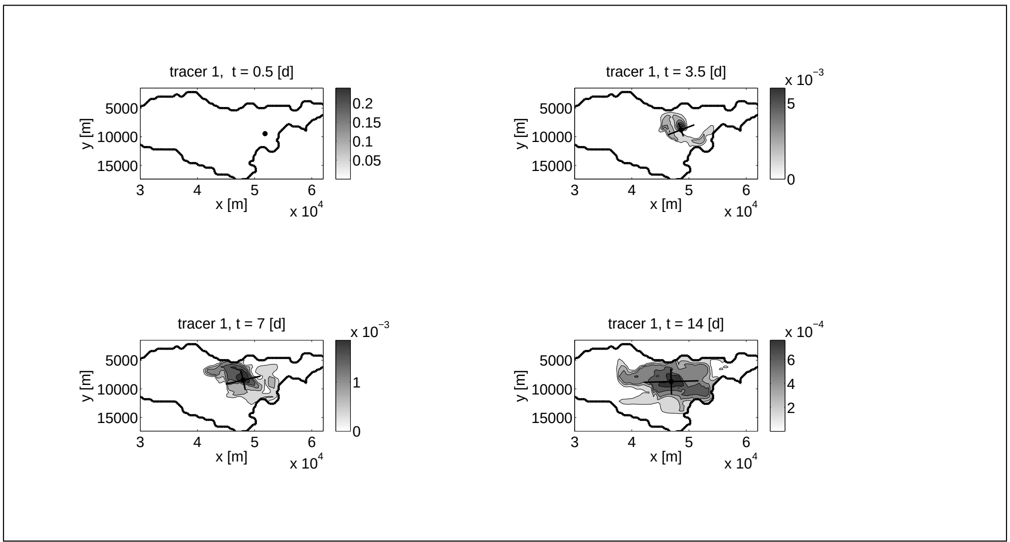

Figure 4.21: Spreading of tracer 1 of simulation 4 in major and minor direction around the centre of mass and concentration field for different time steps.

are not strongly developed yet. So the characterisation of the tracer cloud using the spatial moment analysis matches quite good up to that point. Afterwards it depends on the special situation for each tracer.

In figures 4.21 to 4.23 tracer experiments with release points with a distance between 2 and 3.5 kilometres to one shore are shown. As expected the tracer clouds reach the shore in a shorter time than the clouds of tracers released in a central position in the lake, in most experiments already after 3 or 4 days (here fig. 4.22 and 4.23). A special situation can be seen in figure 4.21 where the cloud is transported away from the shore and towards the centre of the lake by the flow. In that case it can be seen that with increasing distance from the coast the approximation using the moment analysis as explained before fits better. Usually, the effects of the lake boundaries are stronger if the tracer is released closer to the shore. In figure 4.22 and 4.23 it can be seen that the approximation fits quite well until the tracer cloud reaches the coast after 4 days. Afterwards it is getting more difficult because in most cases the tracer distribution is stretched along the shore by the flow. This effect can be seen even more clearly in figures 4.24 and 4.25 where the tracer is released directly at the lake boundary. For those cases it is almost impossible to use the spatial moment analysis for the approximation of the tracer cloud. In figure 4.23 additionally the effect of separation of the tracer cloud as described in the previous paragraph occurs. In this case the estimation by using the results of the moment analysis begins to fail after 7 days and totally fails at the latest after day 14, as can be seen.

Finally, a tracer released close to Lake Überlingen is considered (fig. 4.26). Up to day 7 the cloud resulting from the moment analysis can express the real tracer distribution in a sufficient way. It can be observed that the cloud moves in a north west direction and reaches the north west boundary approximately after 7 days. Until day 14 the tracer moves further north west along the boundary and arrives in Lake Überlingen. At the border between the main basin of Lake Constance and Lake Überlingen the width of the cross section is nearly halved. The tracer distribution that follows from this geometry produces another problem for the approximation using the results of the

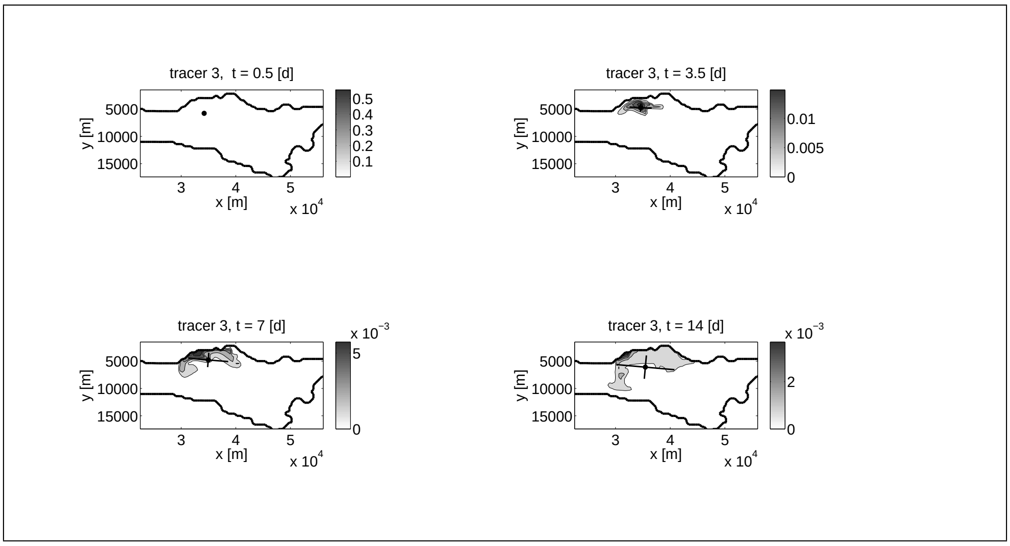

Figure 4.22: Spreading of tracer 3 of simulation 2 in major and minor direction around the centre of mass and concentration field for different time steps.

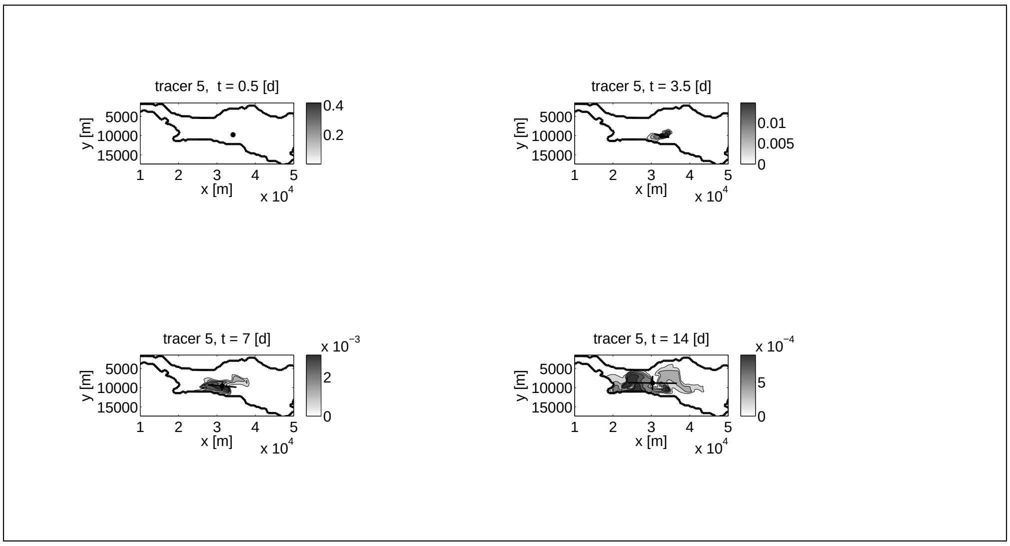

Figure 4.23: Spreading of tracer 5 of simulation 2 in major and minor direction around the centre of mass and concentration field for different time steps.

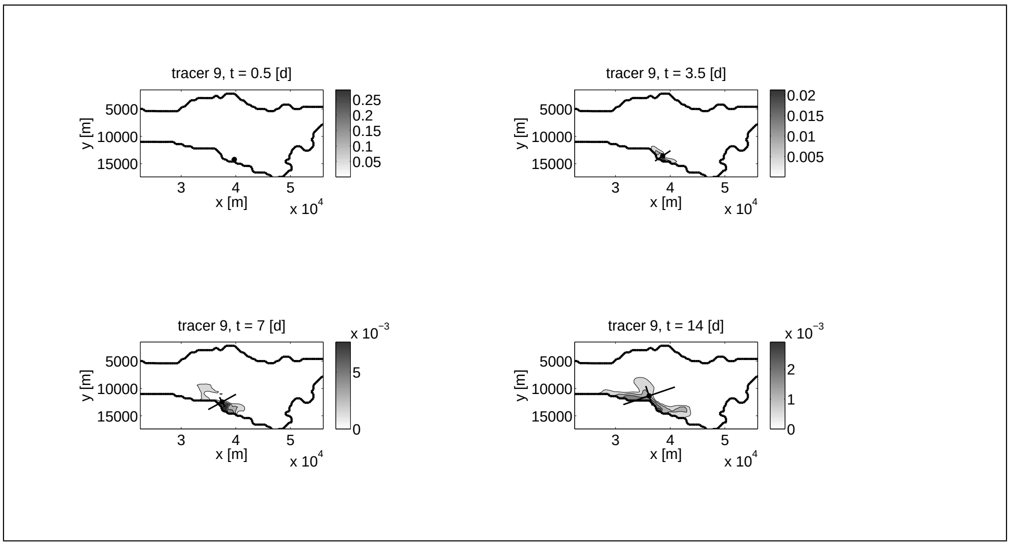

Figure 4.24: Spreading of tracer 9 of simulation 2 in major and minor direction around the centre of mass and concentration field for different time steps.

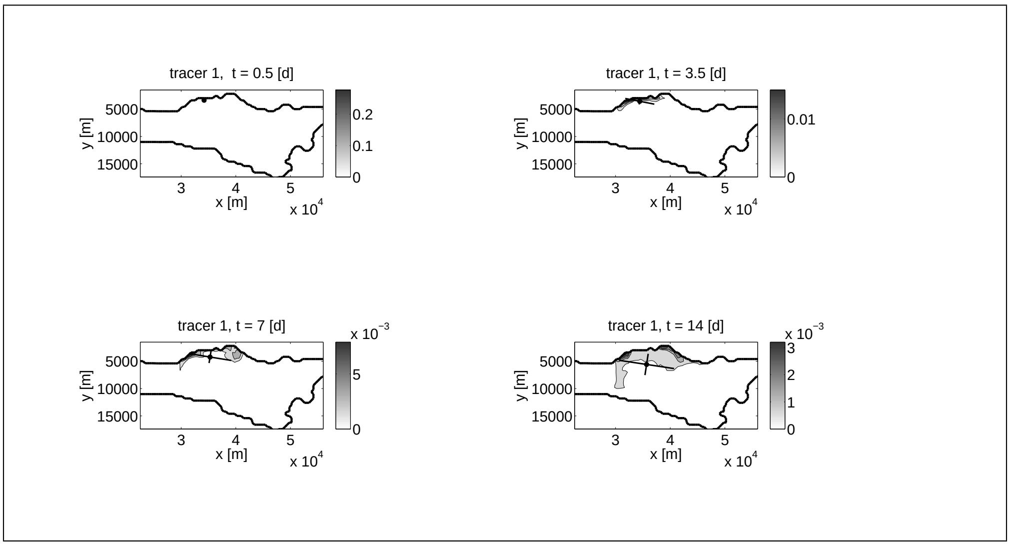

Figure 4.25: Spreading of tracer 1 of simulation 2 in major and minor direction around the centre of mass and concentration field for different time steps.

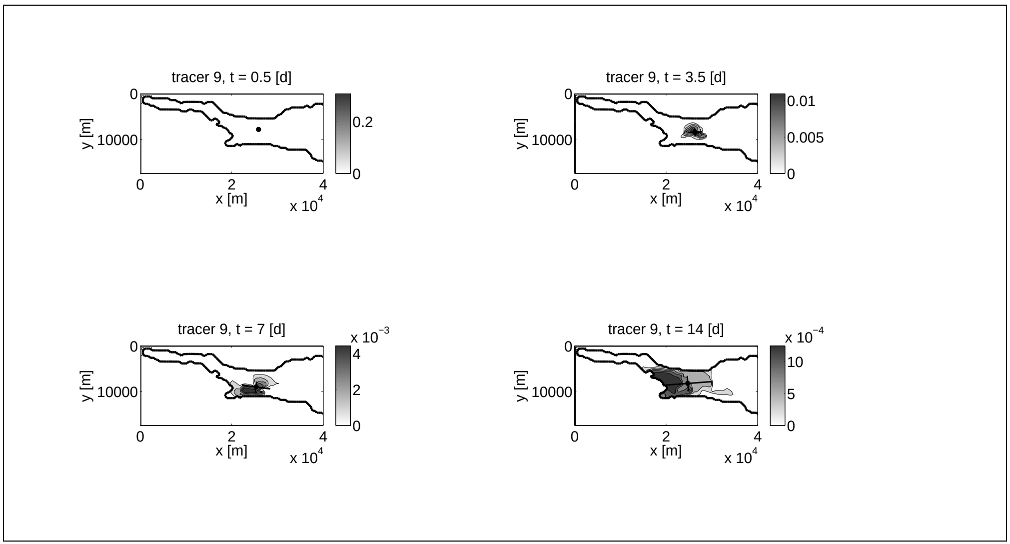

Figure 4.26: Spreading of tracer 9 of simulation 4 in major and minor direction around the centre of mass and concentration field for different time steps.

moment analysis. Thus as can be seen, the passage to Lake Überlingen is not noticed by the spatial moments.

Recapitulating, the spatial moments can be a good method to simplify a complex situation and to analyse complex data. But they have to be used in a careful way. If the situation is as complex as in Lake Constance the approximation can be quite good but also quite poor. The applicability strongly depends on the local as well as on the large scale situation. If the effects of boundaries and of separation of the tracer cloud are small, good estimations can be achieved by the method of spatial moments. For Lake Constance that means if a tracer is released in a sufficient distance to the shore ($\approx$ 2 km) the spatial moments are a good approximation up to 4 days. Up to 7 days the approximation is still good if a tracer is released far away from the shore in the centre of the lake and also sufficiently good for a release in a distance between 2 and 3.5 kilometres from the coast. After one week effects of large scale advection become stronger which could be separation of the tracer cloud or the stretching along large scale circulating flow and also the influences of the lake boundaries are not negligible any longer. Tracers which are injected next to the shore can not be approximated by the method of spatial moments in a sufficient way. A very special situation can be found when looking at the transport of a tracer from Lake Constance into Lake Überlingen. Here it is shown that the moment analysis can not be used to get reliable information whether the tracer is transported from Lake Constance into Lake Überlingen or not.

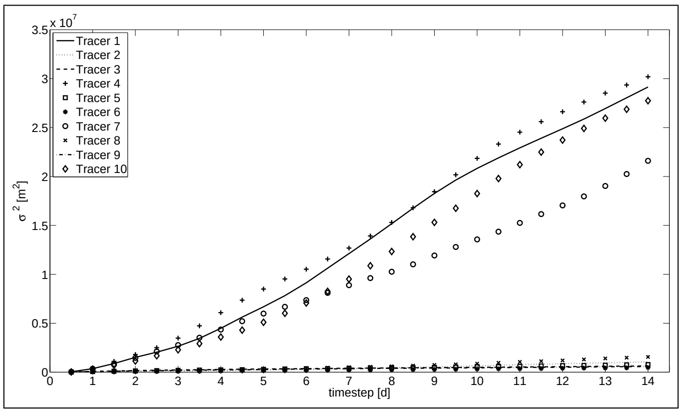

Figure 4.27: Growth of the tracer clouds of simulation 3 over time.

4.4 Behaviour of the cloud size

The key point of the moment analysis is the behaviour of the cloud size. As explained in chapter 2.1 the cloud size can be calculated from the moments using equations 2.4 and 2.5. Once a functional relationship for the behaviour of the cloud size is known for example a diffusivity can be calculated according to equation 2.6. To establish a relationship horizontal diffusion models can be used. In the following, the behaviour of the cloud size of the numerical tracer experiments in Lake Constance is analysed especially concerning boundary influences. Afterwards the application of the introduced models for horizontal diffusion (ch. 2.2) will be described.

4.4.1 Boundary influences

At first, this section focuses on the depth dependence of the growth of a tracer cloud. Figure 4.27 shows the development of the cloud size over time for several tracers. Tracers 2, 3, 5, 6, 8 and 9 are released in deeper layers of Lake Constance (table 3.1) whereas tracers 1, 4, 7 and 10 are injected close to the surface. As shown before, the effect of spreading is very small in the deeper areas of a stratified lake. This can also be seen in the growth of the tracer cloud over time. For the tracers released in higher depth the cloud size is almost constant compared to the ones released at the surface. So it is shown again that no appreciable mixing takes place in the deeper layers of a stratified lake. Therefore, all following considerations focus on tracers released close to the surface.

In figure 4.28 tracers of all four simulations are shown. As can be seen the curves of the growth of the cloud size vary in a wide spectrum. There are three groups: tracers released in centre of the lake, tracers released at a distance of 2 to 3.5 kilometres to the shore and tracers released close to the shore. The growth of the clouds released in the centre is the strongest whereas that of the ones released close to the shore is the smallest. The growth of the clouds of the tracers released in a distance of 2 to 3.5 kilometres to the shore lies in between. Most of the curves tend to have an inflexion point which means that the growth is retarded or accelerated from that point in time on. A reason for acceleration can be spreading due to large scale advection. The main reason for retardation is influence of the lake boundary. As shown in chapter 4.3 all tracer clouds reach the shore after one week at the latest. For most clouds this can

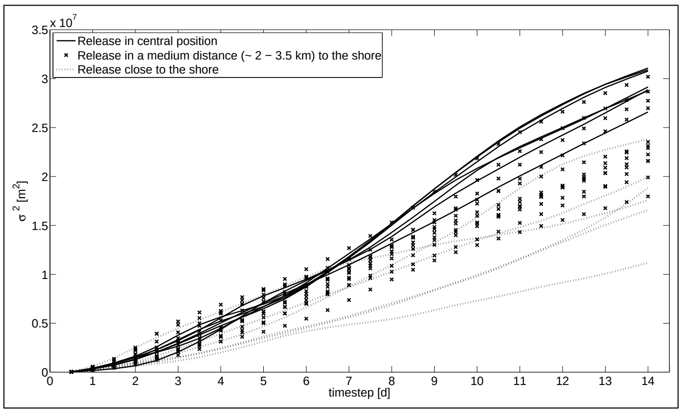

Figure 4.28: Growth of the tracer clouds of tracers released in different distances to the shore over time.

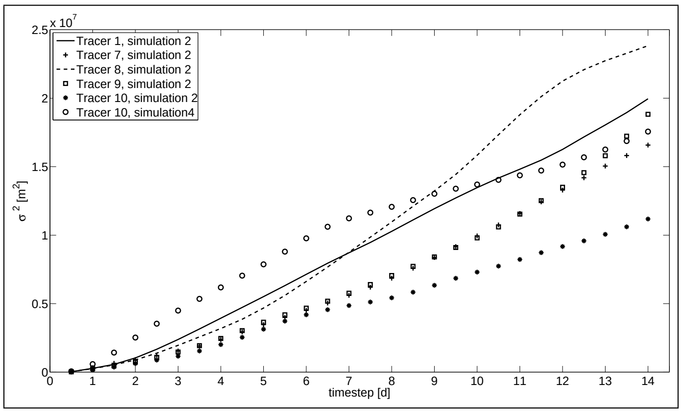

Figure 4.29: Growth of the tracer clouds of tracers released close to the shore over time.

also be observed looking at the behaviour of the cloud size over time which shows a retardation of the growth after approximately 7 days.

When looking at the behaviour of the clouds of tracers released close to the shore as can be seen in figure 4.29 the curves look different. Some show more than one inflexion point and some show now inflexion point at all. The growth seems to be almost linear and slow compared to the tracers released in central position (fig. 4.28). After 14 days the cloud size varies between 1.1 x 10^7 m^2 (11 km^2) and 2.4 x 10^7 m^2 (24 km^2) which means a difference of 13 km^2. It was already shown above that the moment analysis is not able to describe tracer clouds of tracers released close to the shore in a sufficient way (ch. 4.3). The same is true for the consideration of the cloud size over time. It can be clearly shown that the boundary retards the growth of the tracer cloud, which is of a factor 3 smaller than a cloud of a tracer released in the centre of the lake, after 14 days.

Considering the growth of the clouds of tracers released at a distance of 2 to 3.5 kilometres to the shore a similar behaviour to the tracer experiments discussed above can be noticed at first (fig. 4.30). Compared to the previous case however almost all curves seem to have more than one inflexion point. Another difference is that the behaviour of the cloud sizes changes between 7 and 8 days. Before this the curves run rather parallel, afterwards the range is widening. In the time period between day 3

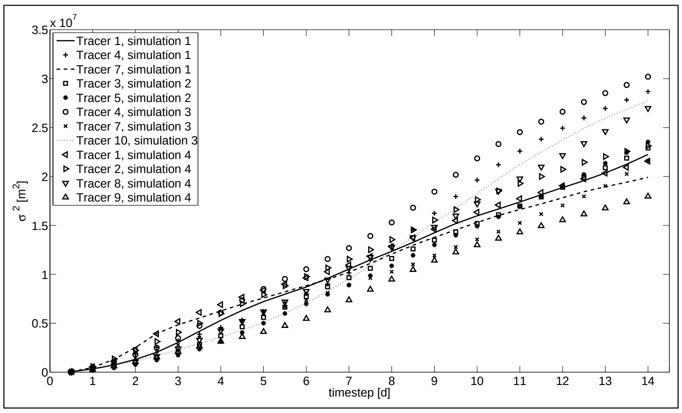

Figure 4.30: Growth of the tracer clouds of tracers released in a distance of 2 - 3.5 km to the shore over time.

and day 8 a first inflexion point can be found for almost all the tracers. Combined with the results of chapter 4.3 it can be interpreted as the period in which the lake boundaries begin to noticeably affect the growth of the cloud size by retardation. After 7 days the differences between the curves of the cloud size increase as the effects of the shore are not the same for the different release points. Additionally, the effects of larger scale advective motion become apparent after approximately one week as described in chapter 4.3 which also affect the different tracer clouds in different ways. After 7 days the cloud size varies between 0.7 x 10^7 m^2 (7 km^2) and 1.3 x 10^7 m^2 (13 km^2) which means a difference of 6 km^2, after 14 days a difference of 14 km^2 can be observed, which is then comparable to the tracers released close to the shore.

Finally, figure 4.31 shows the development of the cloud size over time for tracers released in the centre of Lake Constance. As can be seen all these tracers show a very similar behaviour. There is an exponential growth of the cloud size up to day 7 where an inflexion point can be identified. Afterwards the growth is retarded, which seems reasonable as the tracer cloud reaches the shore after approximately one week (ch. 4.3). The cloud size after 7 days varies in a range of 2 10^6 m^2 which corresponds to 2 km^2, after 14 days between 2.7 x 10^7 m^2 (27 km^2) and 3.2 x 10^7 m^2 (32 km^2) which means a difference of 5 km^2. This shows that the situations for the different tracers released in central positions of Lake Constance are quite comparable, at least before they reach the shore after one week. Afterwards, the differences are still relatively small until day 14 compared to the cases discussed above, in which the boundary influences are much stronger.

4.4.2 Applicability of horizontal diffusion models

In the previous section it was shown that for tracers released into Lake Constance in a central position a similar behaviour can be observed (fig. 4.31). These tracer experiments are now compared to the different diffusion models described in chapter 2.2. As the models are valid until a tracer cloud reaches a shore only the first 7 days of the tracer experiments are considered. The parameters A_1 to A_k of a specific model with the modelled cloud size $\sigma^2_{mod}(t_i, A_1, \ldots, A_k)$ are adjusted using a least squares fit.

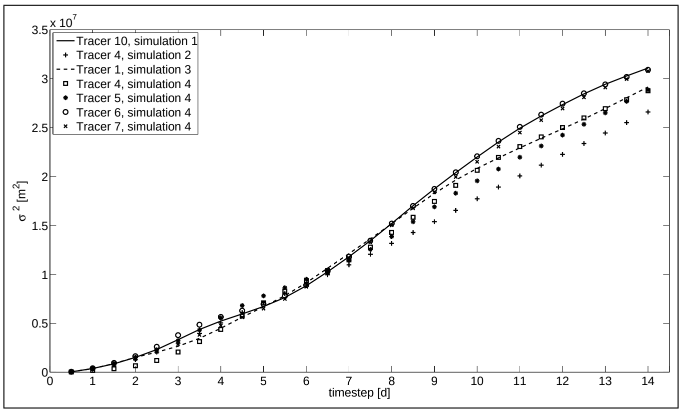

Figure 4.31: Growth of the tracer clouds of tracers released in the centre of the lake over time.

Quality of a model fit

A χ^2 test according to *Peeters et al.* [1] is used to check if the modelled cloud size is compatible to the data of the simulations. Therefore the quantity

$$\chi^2 \equiv \sum_{i=1}^{n} \left(\frac{\sigma_i^2 - \sigma_{mod}^2(t_i, A_1, \ldots, A_k)}{w_i} \right)^2 \tag{4.1}$$

is calculated where w_i is the absolute error of the cloud size σ^2 and $i = 1, \ldots, n$ are the different output time steps of the simulation. For the calculation of w_i a relative error of σ^2 of 20% is assumed for all time steps but t_0. In the simulation the tracer is released into one computational cell at t_0 which means into an volume of 0.4 km^3 immediately. So the cloud size is far away from zero at the beginning. Then the growth should usually start slowly and increase with time. So another problem could show up at the beginning when the cloud size is in the order of a computational cell. Growing inside the neighbour cell the size of a tracer cloud could immediately double from one time step to the next. Therefore for t_0 the relative error of the cloud size is assumed to be 100% which damps the effect of the systematical error, done in the models at low time steps, in the χ^2 test. The variable χ^2 is supposed to be χ^2 distributed with k degrees of freedom, where k is the difference between the number of fitting parameters and the number of data points of the simulations. Here 14 points in time are considered meaning that the degree of freedom for the two-parameter models is 12 and for the three-parameter models is 11. A model is rejected if the probability of χ^2 to be larger than or equal to χ^2_{mod} is less than 1 %. That means that for $k = 11$, χ^2_{mod} has to be compared with $\chi^2 = 24.73$ and for $k = 12$ with $\chi^2 = 26.22$.

The inertial subrange model

According to equation 2.12 the power law $\sigma^2 = A_1 t^{A_2}$ is fitted yielding to A_1 and A_2 for the different tracer experiments as can be found in table 4.1. According to the inertial subrange model (eq. 2.10) the cloud size should grow with time as t^3. Though the fitting gives values for the exponent A_2 between 1.2 and 1.7 for the results of the simulations which is clearly different to the exponent 3 of the inertial subrange model.

Thus, a model $\sigma^2 = \text{const}\, t^3$ has to be rejected. According to the χ^2 test the power law fit with the parameters of table 4.1 is acceptable for all of the seven tracer experiments.

As in the tracer experiments there is a finite cloud size at $t = 0$ the above power law model is extended by a third fitting parameter A_3 where $t = -|A_3|$ can be interpreted as the hypothetical release time when the cloud size was zero. Fitting the cloud size to the model $\sigma^2 = A_1(t + |A_3|)^{A_2}$ yields exponents of A_2 between 1.2 and 1.9, which is also not compatible with a growth of the tracer cloud proportional to the time to the power of 3. An extended approach of the inertial subrange model $\sigma^2 = A_1(t + |A_2|)^3$ was also fitted directly. Both the comparison of the exponents as well as the χ^2 test for the inertial subrange model (table 4.1) show clearly that also the extended inertial subrange model can not be verified. However, concerning the χ^2 test of the fitting of the modified power law model it can be seen that this model shows an acceptable estimation for all tracer experiments. Although an improvement of the fit might be expected due to the extension with the hypothetical release time the results of the χ^2 test are comparable to the simple power law model. Like explained above in section 4.4.2 the data of the simulations show a initial cloud size at $t = 0$, but as this is small compared to the size at later time steps it seems to be negligible concerning the quality of the fitting.

The curves of the fittings discussed in this section are shown in figures 4.32 to 4.38. In these figures it can be seen, too, that the initial subrange model is not a good approximation for the data of the simulations. Differences between the power law approaches with and without a hypothetical release time can only be observed in figures 4.32, 4.34 and 4.38. This is compatible with the results of the χ^2 test (table 4.1).

The Joseph and Sendner model

According to *Joseph and Sendner* a modelled cloud size $\sigma^2 = A_1(t + |A_2|)^2$ would be used, where σ^2 grows with the square of the elapsed time (ch. 2.2). Again a parameter A_2 is used with respect to an initial cloud size. As can be seen in table 4.1 for none of the tracer experiments an exponent of around 2 can be achieved using the extended power low. Only for tracer 1 of simulation 3 does the exponent of 1.814 come close to 2. That means that also the *Joseph and Sendner* model has to be rejected.

The shear diffusion model

Both the inertial subrange model as well as the *Joseph and Sendner* model predict a radially symmetric behaviour. However, previous sections (4.2 and 4.3) show that the spreading of the tracer clouds is usually elongated. This means that an important aspect is missing for the characterisation of a cloud. The big advantage of shear diffusion models is the possibility to describe non-radially symmetric tracer distributions (ch. 2.2). According to equation 2.16 the cloud size can then be modelled as

$$\sigma^2 = 2\sqrt{4A_1^2 t^2 + 1/3\, A_1 A_2 t^4},$$

where $A_1 = K_h$ and $A_2 = K_h(\partial u/\partial y)^2 + 4K_z(\partial u/\partial z)^2$. The growth of the cloud size should be $\sigma \sim t^m$ with m changing from 1 to 2 (ch. 2.2). So the shear diffusion model should be in fair agreement with the results of the simulations, as the considerations using the power laws already showed exponents in this range. The χ^2 test shows that only for 4 out of 7 tracer experiments the fit satisfies the significance criteria. This

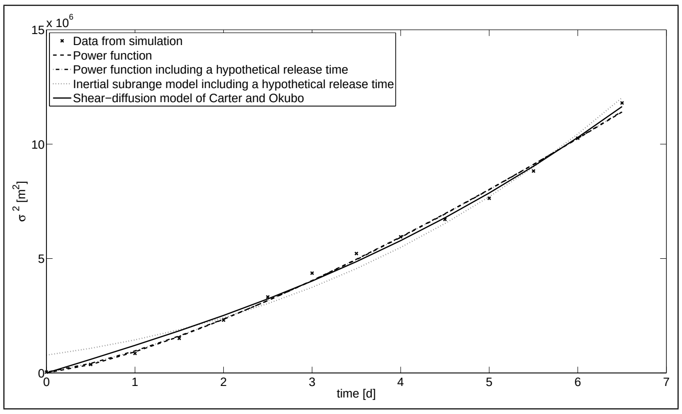

Figure 4.32: Fitted curves and data for the growth of the tracer cloud of tracer 10 of simulation 1.

means that with a probability of approximately 60% the growth of the cloud size of a tracer released into Lake Constance in a central position can be described by a shear diffusion model. Especially the fit of tracer 4 of simulation 4 shows a value of χ^2_{mod} that is significantly higher than $\chi^2 = 26.22$.

Looking at the fitting curves shown by figures 4.32 to 4.38 it can also be noticed that the general power laws show a better approximation of the data of the simulations than the shear stress model. However, it is also shown that the behaviour of the cloud size as $\sigma \sim t^m$ with m lying between 1 and 2 is the same as the behaviour predicted by the shear diffusion model. Furthermore the shear diffusion model is the only one of the described horizontal diffusion models that is able to estimate the growth of the cloud size for tracers released in a central position in a sufficient way in 60% of the cases. Both, the inertial subrange model as well as the *Joseph and Sendner* model fail.

As mentioned before the shear diffusion model describes not only the cloud size but is also able to model the variance in the direction of the major and minor principal axes as function of time (eq. 2.15). The corresponding model functions containing three fitting parameters then look like:

$$\begin{aligned}\sigma^2_{ma} =& 2A_1 t + \frac{1}{3}(A_1 A_2^2 + A_3)t^3 + \\ & \sqrt{A_1^2 A_2^2 t^4 + [\frac{1}{3}(A_1 A_2^2 + A_3)t^3]^2}, \\ \sigma^2_{mi} =& 2A_1 t + \frac{1}{3}(A_1 A_2^2 + A_3)t^3 - \\ & \sqrt{A_1^2 A_2^2 t^4 + [\frac{1}{3}(A_1 A_2^2 + A_3)t^3]^2},\end{aligned}$$

where $A_1 = K_h$, $A_2 = \partial u/\partial x$ and $A_3 = K_z(\partial u/\partial z)^2$ and a point-like initial concentration distribution is assumed. This modelling of the variances in the direction of the major and minor principal axes is not further tested for the simulations of Lake Constance. But *Peeters et al.* [1] showed for several experiments that the shear stress model can also be successfully used to describe the behaviour of the variances in direction of the principal axes.

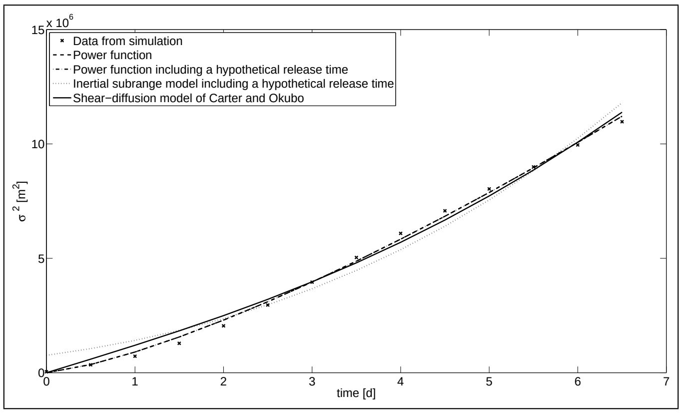

Figure 4.33: Fitted curves and data for the growth of the tracer cloud of tracer 4 of simulation 2.

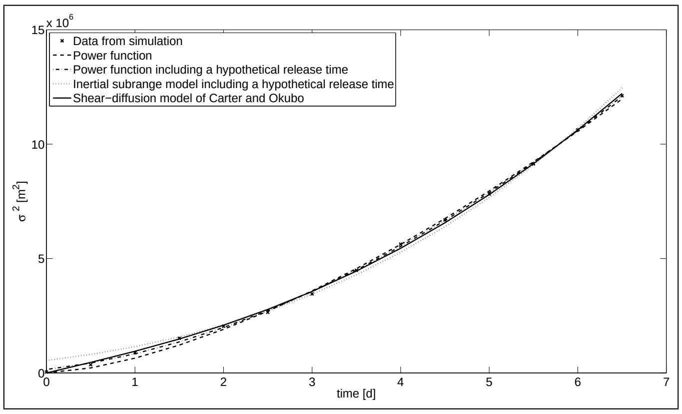

Figure 4.34: Fitted curves and data for the growth of the tracer cloud of tracer 1 of simulation 3.

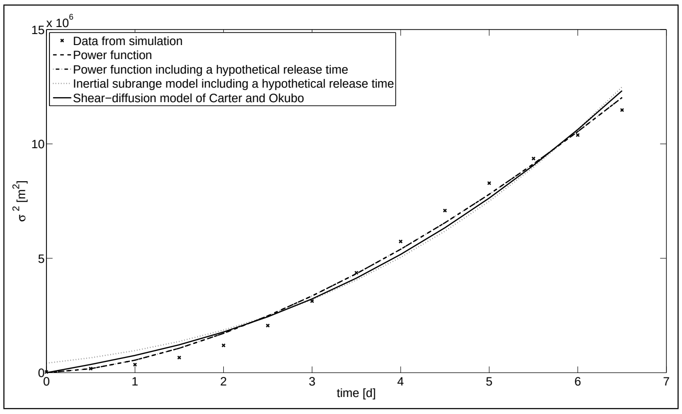

Figure 4.35: Fitted curves and data for the growth of the tracer cloud of tracer 4 of simulation 4.

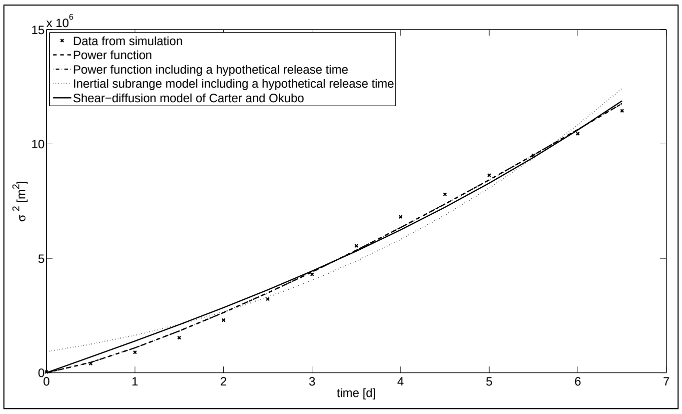

Figure 4.36: Fitted curves and data for the growth of the tracer cloud of tracer 5 of simulation 4.

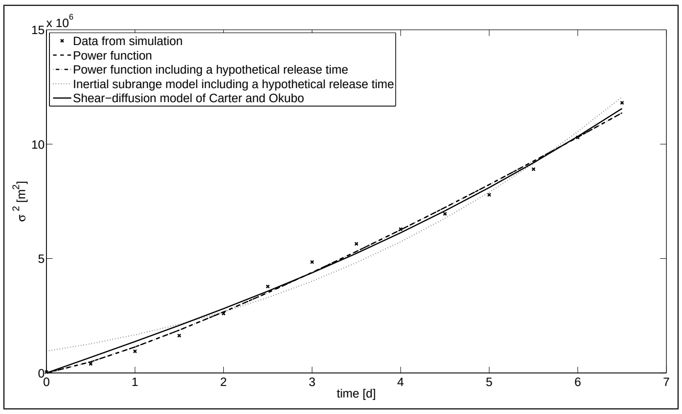

Figure 4.37: Fitted curves and data for the growth of the tracer cloud of tracer 6 of simulation 4.

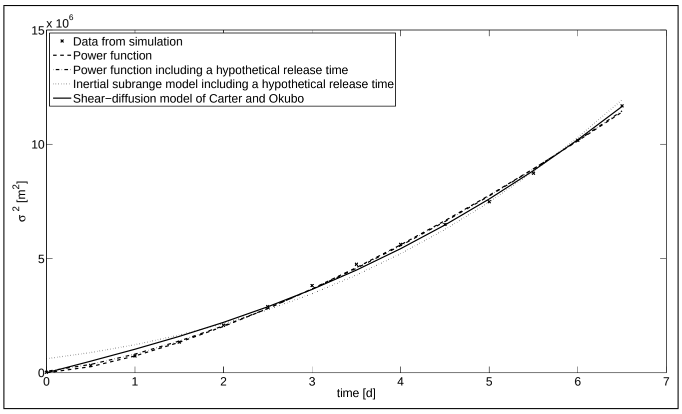

Figure 4.38: Fitted curves and data for the growth of the tracer cloud of tracer 7 of simulation 4.

Simulation	1	2	3	4	4	4	4
Tracer	10	4	1	4	5	6	7
Power function: $\sigma^2 = A_1 t^{A_2}$							
A1 $[m^2/s^{A_2}]$	924445.5	905654.6	647439.1	547251.8	1088836.3	1136873.7	733740.5
A2 [-]	1.342	1.344	1.558	1.651	1.272	1.230	1.466
$\chi^2_{\mathbf{mod}}$	1,66	4,37	7,74	24,57	4,48	4,38	1,91
Power function including A_3 *as parameter for a hypothetical release time:* $\sigma^2 = A_1(t+\|A_3\|)^{A_2}$							
A1 $[m^2/s^{A_2}]$	845269.0	905654.6	342164.3	547251.8	1088836.3	1136873.7	586221.4
A2 [-]	1.380	1.344	1.814	1.651	1.272	1.230	1.559
A3 [s]	-0.0997	6.058×10^{-17}	-0.6376	5.504×10^{-17}	-4.487×10^{-17}	1.264×10^{-17}	-0.2353
$\chi^2_{\mathbf{mod}}$	1,32	4,37	8,53	24,57	4,48	4,38	4,56
Initial subrange model including A_2 *as parameter for a hypothetical release time:* $\sigma^2 = A_1(t+\|A_2\|)^3$							
A1 $[m^2/s^3]$	9402.5	9243.8	12340.2	14206.3	8840.1	8185.0	10805.1
A2 [s]	4.356	4.349	3.532	3.080	4.702	4.882	3.841
$\chi^2_{\mathbf{mod}}$	540,37	442,77	189,83	474,30	854,47	745,83	870,04
Shear-diffusion model applied to cloud size: $\sigma^2 = 2\sqrt{4A_1^2t^2 + 1/3\,A_1A_2t^4}$							
A1 $[m^2/s]$	296780.4	295745.8	228499.6	176078.9	343183.2	340028.4	250877.2
A2 $[m^2/s^3]$	107686.0	100174.7	209493.2	312517.3	75403.9	68536.5	156174.6
$\chi^2_{\mathbf{mod}}$	15,95	31,02	3,24	85,42	27,09	21,26	14,43

Table 4.1: Fitting parameters and modelled χ^2 for the different models.

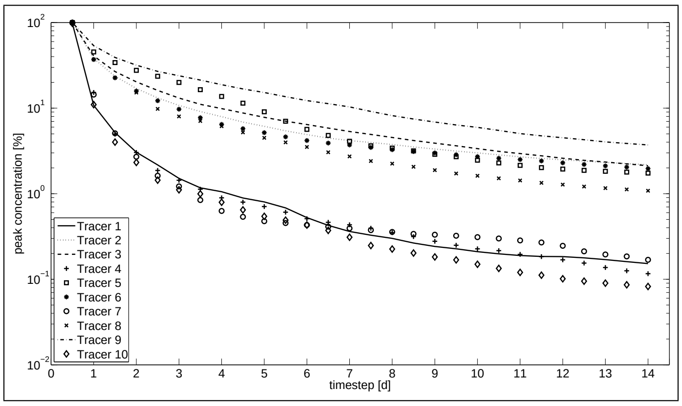

Figure 4.39: Peak concentrations of the tracer clouds of simulation 1 over time.

4.5 Relevance of dilution of the tracer concentration

For the characterisation of a tracer cloud especially concerning its potential of danger not only the spatial distribution but also the rate of dilution is important. Therefore, the temporal behaviour of the peak concentration of a tracer cloud is considered for the different simulations. The results can be seen in figures 4.39 to 4.42. Figures 4.39 and 4.41 clearly show the different behaviour of tracers released at the surface and tracers released into deeper layers where the process of dilution is much slower. The peak concentration of tracers released at the surface is below 1% of the initial concentration after one week, whereas the peak concentration of tracers released at greater depth does not reach the 1% mark within the simulated time of two weeks. Figure 4.40 shows the influence of the distance to the shore on the dilution process. The tracers released at a larger distance (Tracer 4 and 5) show a noticeably faster dilution than the other tracers. After two weeks tracers released between 2 and 5 kilometres to the shore close to the surface show a peak concentration between 0.08% and 0.2%, tracers released close to the shore around 0.4% (figs. 4.39, 4.40, 4.41 and 4.42).
These results show that a substance released in a sufficiently large concentration could still have a notable peak concentration after one week. An initial concentration of 100 mg/l for example which is a reasonable value in case of an accident would still result in a maximum concentration of 1 mg/l. Depending on the substance, that could still be an endangering amount. The consideration of the peak concentration however represents the worst case. Depending on the position within the tracer cloud the concentrations can of course be much smaller. One has to be aware of that the peak concentration is not located in the centre of mass. Finally, it has to be mentioned that only conservative tracers are considered here and so biodegradation has no effect on the decrease of the peak concentration over time.

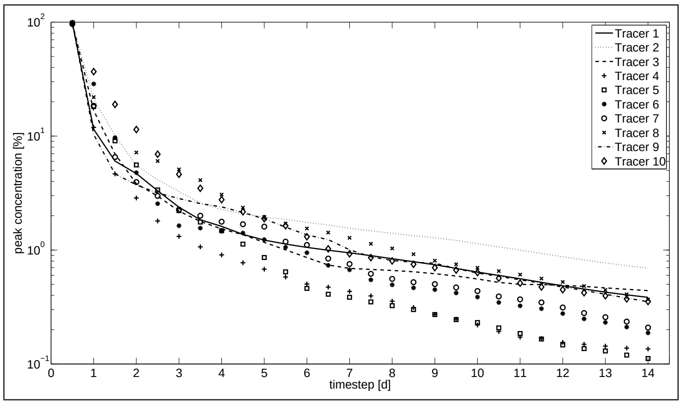

Figure 4.40: Peak concentrations of the tracer clouds of simulation 2 over time.

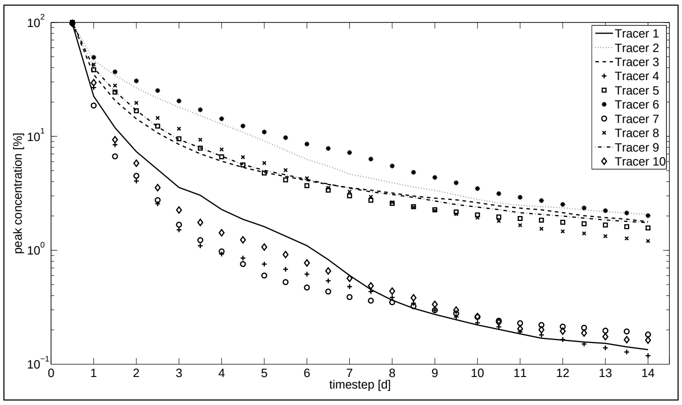

Figure 4.41: Peak concentrations of the tracer clouds of simulation 3 over time.

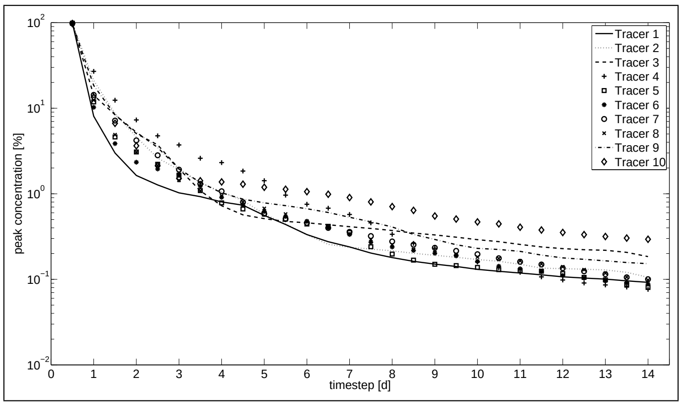

Figure 4.42: Peak concentrations of the tracer clouds of simulation 4 over time.

5 Summary and conclusions

In this study several numerical tracer experiments for Lake Constance were done (ch. 3). The data of the simulations were analysed using the method of spatial moments as described in chapter 2.1. Here the behaviour of a tracer cloud was investigated and the applicability of the moment analyses for Lake Constance was established comparing the approximated cloud shape defined by the moments to the real concentration distribution (ch. 4). Afterwards the behaviour of the cloud size over time was investigated with special regard to boundary influences. In addition, theoretical horizontal diffusion models described in chapter 2.2 were fitted to the data of the simulations. Finally, the process of dilution was considered.

In chapters 4.1 and 4.2 it was shown that the movement of the centre of mass and the spreading around the centre of mass is small in deeper layers compared to the near surface layers of the stratified Lake Constance. Further it was shown that the vertical movement of the centre of mass and the vertical spreading are negligible compared to the horizontal components in a stratified lake.

Considering the movement of the centre of mass (ch. 4.1) a link to the local flow field was investigated. As an important result it appeared that the local velocity field can not be used to estimate the movement of the centre of mass which is a quantity resulting from a spatial averaging process. An evaluation of the change of the centre of mass in connection to the flow situation of Lake Constance can only be done considering the whole area of a tracer cloud and the large scale motions. The analysis of the centres of mass of the different simulations then showed that the main direction of the movement appears to be from the south east to the north west. This is reasonable as this is the direction of the wind which is the main driving force.

Figure 5.1 shows the schematic change of the shape of a tracer cloud released in a central position over time, as investigated in chapter 4.3. As can be seen until day 3.5 the cloud has a nearly elliptic shape which means it can be well approximated by a Gaussian distribution implied by the method of spatial moments. At day 7 still a shape similar to an ellipse can be assumed and an approximation by the method of spatial moments works well. After 7 days effects of large scale advection and of the boundaries begin to affect the shape of the cloud and after 14 days the cloud is widely and irregular spread in several directions. Therefore, after day seven the spatial moments are not able to give an usable approximation of the cloud shape.
For tracers released at a distance between 2 and 3.5 kilometres to the shore this was shown to be valid too (4.3). Although the tracer clouds already reach the boundaries after around 4 days the approximation of the cloud shape after 7 days is still sufficiently good using the moment analysis. For tracers released close to the shore it was shown in chapter 4.3 that an approximation by the methods of spatial moments is not meaningful.

Considering the behaviour of the cloud size it is shown in chapter 4.4 that a sensitiveness to boundary influences can be observed. This means that the growth of a tracer cloud is usually retarded after the cloud reached the shore. For tracers released in the

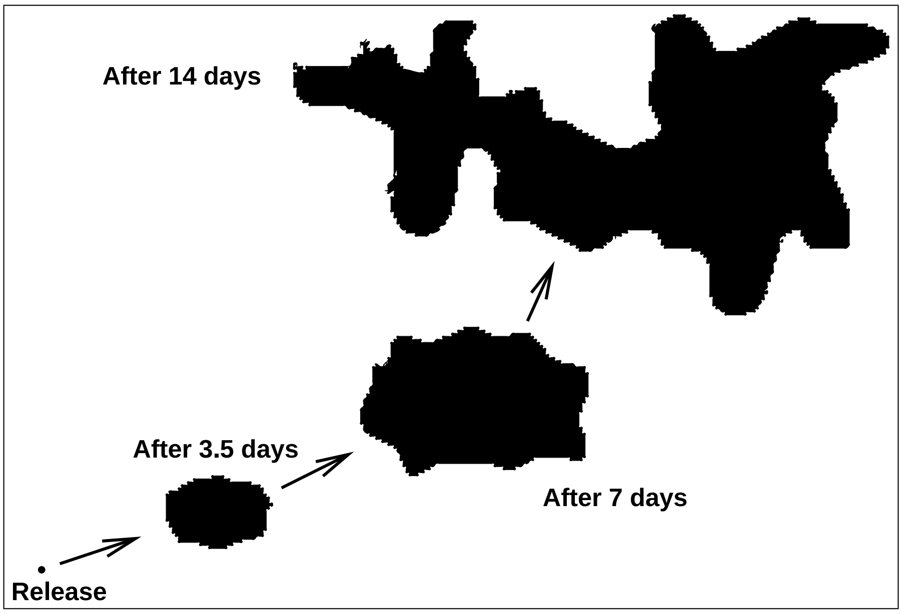

Figure 5.1: Schematic spreading of a tracer cloud in Lake Constance.

centre of the lake with an approximate distance of 5 kilometres this could be observed after 7 days and for tracers released in a distance between 2 and 3.5 kilometres after approximately 4 days.

For tracers released in a central position similar curves describing the growth of the cloud size over time could be found. To investigate this behaviour the horizontal diffusion models described in chapter 2.2 were fitted to these curves. The fitting was done for the first week only to minimise boundary influences. Only the shear diffusion model by *Carter and Okubo* was able to describe the growth of the tracer cloud in a sufficient way and for 60% of the tracers released in the centre of Lake Constance. For the other 40% the fitting failed the χ^2 test (4.4.2). Systematic errors might be caused by the initial cloud size and influences of the discretisation. The inertial subrange model and the model by *Joseph and Sendner* failed always. This might be caused by the assumption of a radially symmetric behaviour.

To describe the process of dilution the peak concentration was considered in chapter 4.5. For tracers released close to the surface a concentration around 1% of the input concentration can be found after 1 week and around 0.1% after 2 weeks. Using that information the maximum possible concentration and therefore a worst case can be estimated.
For example uncertainties in the approximation using spatial moments can then be relativised as on the boundary of a tracer cloud the concentrations are usually much smaller again than the peak concentration.

All results of this study only represent one special situation with an uniform constant wind coming from south east. Anyhow, it has to be kept in mind that the flow and transport situation in Lake Constance is very complex. To get a more general idea of the situation much more analysis for different conditions has to be done. However, it is shown that the method of spatial moments can be applied to Upper Lake Constance yielding to satisfying results as long as boundary influences and influences of large scale advection can be neglected. Furthermore, it was shown that theoretical horizontal diffusion models can describe the behaviour of the cloud size which yields to a good possibility to estimate diffusion coefficients. The applicability of the horizontal diffusion models also depend on the assumption that boundary influences can be neglected. To give a quantitative prediction for the concentration range a consistent behaviour of the peak concentration over time could be established.

Bibliography

[1] **Peeters, F., Wüest, A., Piepke, G. and Imboden, D. M.**
Horizontal Mixing in Lakes; Journal of Geophysical Research, vol. 101, no. C8, pp. 18,361-18,375, 1996

[2] **Imboden, D. M. and Wüest, A.**
Mixing Mechanisms in Lakes; In: Physics and Chemistry of Lakes, Lerman, A., Imboden, D. M., and Gat, J. R. (eds.), Springer, Berlin, pp. 83-138, 1995

[3] **Hodges B. and Dallimore C.**
Manual - Estuary, Lake and Coastal Ocean Model: ELCOM; Centre of Water Research, University of Western Australia, 2006

[4] **Appt, J.**
Analysis of Basin-Scale Internal Waves in Upper Lake Constance; Institute of Hydraulic Engineering, University of Stuttgart, Heft 123, 2003